

Quantum versus classical statistical dynamics of an ultracold Bose gas

Jürgen Berges*

Institut für Kernphysik, Technische Universität Darmstadt, Schlossgartenstrasse 9, 64289 Darmstadt, Germany

Thomas Gasenzer†

Institut für Theoretische Physik, Universität Heidelberg, Philosophenweg 16, 69120 Heidelberg, Germany

We investigate the conditions under which quantum fluctuations are relevant for the quantitative interpretation of experiments with ultracold Bose gases. This requires to go beyond the description in terms of the Gross-Pitaevskii and Hartree-Fock-Bogoliubov mean-field theories, which can be obtained as classical (statistical) field-theory approximations of the quantum many-body problem. We employ functional-integral techniques based on the two-particle irreducible (2PI) effective action. The role of quantum fluctuations is studied within the nonperturbative 2PI $1/\mathcal{N}$ expansion to next-to-leading order. At this accuracy level memory-integrals enter the dynamic equations, which differ for quantum and classical statistical descriptions. This can be used to obtain a 'classicality' condition for the many-body dynamics. We exemplify this condition by studying the nonequilibrium evolution of a 1D Bose gas of sodium atoms, and discuss some distinctive properties of quantum versus classical statistical dynamics.

PACS numbers: 03.75.Kk, 03.75.Nt, 05.30.-d, 05.70.Ln, 11.15.Pg

HD-THEP-07-05

I. INTRODUCTION

The preparation of ultracold atomic Bose and Fermi gases in various trapping environments allows to study in a precise way important aspects of quantum many-body dynamics [1, 2, 3, 4, 5, 6, 7, 8]. For this reason the field has attracted in recent years researchers from a variety of physical disciplines, ranging from condensed-matter to high-energy particle physics and even cosmology. In past experiments with Bose-Einstein condensates of dilute gases it has been found that these are, in many cases, approximately described by a complex scalar field which solves the Gross-Pitaevskii equation (GPE) [9, 10]. Despite the fact that the first-order coherence reflected by this equation has its origin in the quantum nature of the Bose condensation phenomenon, the GPE arises as the classical field-theory approximation of the underlying quantum many-body problem. It thus neglects all quantum statistical fluctuations contributing to the dynamics of the scalar field. However, it is the role of these quantum statistical fluctuations which is of central importance for our quantitative understanding of a wealth of phenomena described by quantum many-body dynamics. Accordingly, experiments which are sensitive to fluctuations are crucial to test our theoretical understanding of complex many-body problems.

If fluctuations are relevant then the quantitative interpretation of the data typically requires nonperturbative theoretical descriptions, which often have to take into account nonequilibrium dynamics to match realistic experimental situations. Two cases should be distinguished in this context: If the real-time dynamics of a Bose gas is dominated by classical statistical fluctuations then it can be well approximated by a large number of numerical integrations of the classical field equation (GPE) and Monte Carlo sampling techniques [11, 12, 13].

This takes into account nonperturbative dynamics, however, neglects all quantum corrections. A corresponding classical statistical description does not exist for fermions. The other case concerns dynamics where quantum fluctuations are relevant. It is an important challenge to quantitatively determine the role of quantum fluctuations, thus predicting signatures for the detection of genuine quantum effects in an experiment. Here, we address this question for a Bose gas.

In fact, many experiments concerning ultracold Bose gases fall short of being sensitive to quantum statistical fluctuations, and can be accurately described by the GPE. The importance of classical statistical fluctuations can rise if the gas is sufficiently dense. A combination of low densities and strong self-interaction can lead to enhanced quantum fluctuations as compared to classical statistical fluctuations. Zero-energy scattering resonances, particularly the so called magnetic Feshbach resonances [14, 15, 16, 17, 18] so far have played a leading role in the creation of strong interactions in degenerate atomic quantum gases. Near a Feshbach resonance, the scattering of, e.g., a pair of Bose-condensed atoms, whose relative energy is very close to zero, can be described by a strongly enhanced s -wave scattering length a . Present-day experimental techniques allow for resonance-enhanced scattering lengths larger than the mean interatomic distance $(N/V)^{-1/3}$ in the gas. As a consequence, the diluteness parameter $a^3 N/V$ is larger than one. The Bose-Einstein condensate is no longer in the collisionless regime, it represents a strongly interacting system. Feshbach resonances have gained a strong practical importance for fermionic gases, where losses are suppressed in the unitary limit [19] and where they allow to study the transition from a phase of Bose-condensed molecules to a BCS type superfluid [6, 8, 20, 21].

One- and two-dimensional traps [22, 23] as well as optical lattices [24, 25] allow to realize strongly correlated many-body states of atoms. In an optical lattice, strong effective interactions can be induced by suppressing the hopping between adjacent lattice sites and thus increasing the weight of the interaction relative to the kinetic energy [24, 26]. This

*email: Juergen.Berges@physik.tu-darmstadt.de

†email: T.Gasenzer@thphys.uni-heidelberg.de

leads, in the limit of near-zero hopping or strong interactions, to a Mott-insulating state [27]. In a one-dimensional trap, the gas enters the so-called Tonks-Girardeau regime, if the dimensionless interaction parameter $\gamma = g_{1D}mV/(\hbar^2N)$ is much larger than one [28, 29, 30]. Here, g_{1D} is the coupling parameter of the one-dimensional gas, e.g., $g_{1D} = 2\hbar^2a/(ml_{\perp}^2)$ for a cylindrical trap with transverse harmonic oscillator length l_{\perp} . In the Tonks-Girardeau limit $\gamma \rightarrow \infty$ the atoms can no longer pass each other and behave in many respects like a one-dimensional ideal Fermi gas [23].

The theory of the full nonperturbative real-time quantum dynamics is in general a demanding problem. Already the description of weakly correlated many-body dynamics suffers from the problem that it requires summations of infinite series of perturbative processes. These summations can be efficiently taken into account using functional-integral techniques for the quantum field theory, which are based on the two-particle irreducible (2PI) effective action [31, 32, 33]. Much progress has recently been achieved using nonperturbative expansions of the 2PI effective action to next-to-leading order in the number of field components [34, 35]. This has been employed in the context of ultracold quantum gases in Ref. [36, 37, 38]. It has previously been successfully used to study far-from-equilibrium dynamics and thermalization in relativistic bosonic [34, 39, 40, 41] and fermionic [42, 43] theories. For an introductory review see Ref. [44]. In Ref. [45] the approach has been used to compare quantum and classical statistical nonequilibrium dynamics for a relativistic scalar field theory in the absence of a field expectation value. Since the dynamic equations for the quantum and classical correlation functions differ only by few characteristic terms, this can be used to derive a 'classicality' condition for many-body dynamics [45, 46].

Here we extend the analytic discussion including a non-zero macroscopic field and apply it to a non-relativistic theory for an ultracold gas with, in the quantum case, bosonic statistics. For our comparison of quantum and classical dynamics we employ the functional-integral approach of the 2PI effective action. We recall that the difference between the quantum and classical statistical theory can be expressed in terms of interaction vertex terms for the quantum theory which are absent in the classical statistical theory. As a consequence, the classical generating functional is characterized by an important reparametrization property, which allows one to scale out the dependence of the dynamics on the scattering length a . As a consequence, for the classical dynamics the effects of a larger self-interaction can always be compensated by a smaller density. It is shown that quantum corrections violate this invariance property. They become of increasing importance with growing scattering length or reduced density. This is used to derive a condition which may be used for experimenters to find signatures of quantum fluctuations when preparing and probing the dynamics of ultracold gases. This condition is not based on thermal equilibrium assumptions and holds also for far-from-equilibrium dynamics. As an application, we study the thermalization of a homogeneous one-dimensional ultracold Bose gas starting from a far-from-equilibrium initial state following Ref. [36]. We compare quantum and classical evo-

lution and demonstrate the validity of our criterion for the nonequilibrium quantum field theory to be well approximated by its classical counterpart. To round off the analysis we discuss some distinctive properties of quantum versus classical statistical dynamics. For instance, the decay of correlations with the initial state happens faster in the classical statistical theory for the one-dimensional Bose gas. Including quantum corrections the system remembers longer the details about the initial conditions.

The use of functional methods to describe the dynamics of classical correlations dates back to the work of Hopf in the context of statistical hydrodynamics [47]. A field theory for the description of classical fluctuations in terms of noncommutative classical fields was first suggested by Martin, Siggia, and Rose (MSR) [48] and has been extensively used in critical dynamics near equilibrium [49]. This theory has been reformulated later in terms of Lagrangian field theory employing functional methods [50, 51, 52, 53, 54, 55]. In these field theoretical approaches to classical statistics, a doubling of the degrees of freedom occurs. For example, in the generating functional for Green's functions, besides each field appearing in the fundamental Lagrangian, a second 'response' field is integrated over. The functional integral approach to quantum field dynamics developed by Schwinger and Keldysh employs a closed time path (CTP) contour [56, 57] in the time-ordered exponential integral. The doubling of fields in the MSR and Lagrangian approaches to classical dynamics corresponds to the fields evaluated separately on the two branches of the Schwinger-Keldysh CTP [58, 59, 60]. Implications of the differences between the classical and quantum vertices, similar to the case considered in this article, have been discussed, for other theories, e.g. in Refs. [60, 61, 62, 63, 64, 65, 66].

Our article is organized as follows: In Section II we recall the functional description of quantum as well as classical statistical non-equilibrium dynamics and use this to construct the respective 2PI effective actions. We then derive the time evolution equations and compare the nonperturbative expansion in the numbers of field components to next-to-leading order for the non-relativistic quantum and classical statistical theory. In Section III we present numerical results for the quantum and classical evolutions of an ultracold one-dimensional Bose gas. Our conclusions are drawn in Section IV. In an appendix we provide some details of employed initial-state density matrices.

II. CLASSICAL VERSUS QUANTUM DYNAMICS OF AN INTERACTING GAS

We consider an ultracold gas of atoms with bosonic statistics. At sufficiently large phase-space densities the system can undergo a phase transition and form a Bose-Einstein condensate, given that dimensionality and trapping geometry fulfill the necessary conditions. For a dilute gas, i.e., if the atomic distance is much smaller than the characteristic length scale of the interactions, typically the s -wave scattering length a , the system may be described by a complex scalar field theory.

We consider such a non-relativistic quantum field theory for

a complex-valued field $\varphi(x)$. This fluctuating field is characterized by the Lagrangian density

$$\begin{aligned} \mathcal{L}(x) = & \frac{i}{2} [\varphi^*(x) \partial_{x_0} \varphi(x) - \varphi(x) \partial_{x_0} \varphi^*(x)] \\ & - \frac{1}{2m} \partial_i \varphi^*(x) \partial_i \varphi(x) - V(x) \varphi^*(x) \varphi(x) \\ & - \frac{g}{2} (\varphi^*(x) \varphi(x))^2 \end{aligned} \quad (1)$$

in the defining functional integral for correlation functions as described below. We use units where $\hbar = 1$. The space-time variable is $x = (x_0 = t, \mathbf{x})$. It is summed over double indices $i = 1, \dots, d$ for d spatial dimensions and $\partial_i \equiv \partial/\partial x_i$. Here V denotes an external potential, and g a real-valued coupling constant. The Euler-Lagrange equation of motion derived from (1) reads

$$i \partial_{x_0} \varphi(x) = \left[-\frac{\partial_i^2}{2m} + V(x) + g|\varphi(x)|^2 \right] \varphi(x). \quad (2)$$

In the context of the physics of quantum gases of indistinguishable Bosons, Eq. (2) is the well known Gross-Pitaevskii equation if the fluctuating field $\varphi(x)$ is identified with its quantum statistical average $\langle \varphi(x) \rangle$ [9, 10]. This equation approximately describes the time evolution of an inherently quantum system, a Bose-Einstein condensed ultracold gas, neglecting all quantum statistical fluctuations contributing to the dynamics of the scalar field. As such, the Gross-Pitaevskii equation is a classical field equation and the inclusion of quantum and statistical fluctuations beyond the classical field approximation is described in the following.

For this we recall in this section the field theoretical formulation of the many-body quantum and classical statistical time evolution. This gives that the dynamic equations for correlation functions differ only by certain terms in the quantum equations which are absent in the classical ones. As a side result, one recovers that the dynamics in the Hartree-Fock-Bogoliubov (HFB) [67, 68, 69] approximation is the same for quantum and classical statistical descriptions for same initial conditions. Moreover, the differences between the quantum and classical dynamical equations are identified in the non-perturbative 2PI $1/\mathcal{N}$ approximation which goes far beyond HFB.

While the field in Eq. (1) is assumed to be complex-valued, we will, in the following, switch to a representation of the field in terms of its real and imaginary part, $\varphi = (\varphi_1 + i\varphi_2)/\sqrt{2}$, where the classical action reads [36]

$$\begin{aligned} S[\varphi] = & \frac{1}{2} \int_{xy} \varphi_a(x) i G_{0,ab}^{-1}(x,y) \varphi_b(y) \\ & - \frac{g}{8} \int_x \varphi_a(x) \varphi_a(x) \varphi_b(x) \varphi_b(x), \end{aligned} \quad (3)$$

with $\int_x \equiv \int dx_0 \int d^d x$. The free classical inverse propagator is given by

$$i G_{0,ab}^{-1}(x,y) = \delta(x-y) [-i\sigma_{ab}^2 \partial_{x_0} - H_{1B}(x) \delta_{ab}], \quad (4)$$

where $H_{1B}(x) = -\partial_i^2/2m + V(x)$ denotes the single-particle Hamiltonian with interaction potential $V(x)$ and

$$\sigma^2 = \begin{pmatrix} 0 & -i \\ i & 0 \end{pmatrix} \quad (5)$$

the Pauli matrix in field-index space. Summation over double indices $a, b, c, \dots = 1, 2$ is implied. Many of the following formal derivations are independent of the detailed form (4) of G_0^{-1} and, in particular, equally valid for relativistic field theories. Note however that as G_0^{-1} in Eq. (4) contains only a first-order time derivative, the canonically conjugate field, in the non-relativistic theory, is

$$\pi_a(x) = \frac{\delta S[\varphi]}{\delta(\partial_{x_0} \varphi_a(x))} = i\sigma_{ab}^2 \varphi_b(x), \quad (6)$$

in contrast to the relativistic case where the canonical momentum equals the time derivative of the field.

A. Quantum statistical dynamics

1. Generating functional

For a given initial-state density matrix $\rho_D(t_0)$, which may characterize a system also far from equilibrium, all information about the quantum field theory is contained in the generating functional for correlation functions:

$$\begin{aligned} Z[J, K; \rho_D] = & \text{Tr} \left[\rho_D(t_0) \mathcal{T}_C \exp \left\{ i \left(\int_{x,c} J_a^C(x) \Phi_a(x) \right. \right. \right. \\ & \left. \left. \left. + \frac{1}{2} \int_{xy,c} \Phi_a(x) K_{ab}^C(x,y) \Phi_b(y) \right) \right\} \right], \end{aligned} \quad (7)$$

with Heisenberg field operators $\Phi_a(x)$ which obey for the non-relativistic theory the commutation relations

$$[\Phi_a(t, \mathbf{x}), \Phi_b(t, \mathbf{y})] = -\sigma_{ab}^2 \delta(\mathbf{x} - \mathbf{y}). \quad (8)$$

In Eq. (7), \mathcal{T}_C denotes time-ordering along the closed time path \mathcal{C} leading from the initial time t_0 along the real time axis to some arbitrary time t and back to t_0 , with $\int_{x,c} \equiv \int_{\mathcal{C}} dx_0 \int d^d x$. Contour time ordering along this path corresponds to usual time ordering along the forward piece \mathcal{C}^+ and antitemporal ordering on the backward piece \mathcal{C}^- . Note that any time on \mathcal{C}^- is considered later than any time on \mathcal{C}^+ . The source terms in Eq. (7) allow to generate correlation functions by functional differentiation such as

$$\langle \mathcal{T}_C \Phi(x_1) \cdots \Phi(x_n) \rangle = \frac{\delta^n Z[J, K; \rho_D]}{i^n \delta J(x_1) \cdots \delta J(x_n)} \Big|_{J,K=0}, \quad (9)$$

where the field indices have been suppressed and we have used that for the closed time path $Z = 1$ in the absence of sources. We have introduced, in Eq. (9), two contour source terms, J^C and K^C , which we use below to go over by Legendre transformation to the corresponding 2PI effective action.

2. Functional integral

For a theory with action (3) the generating functional $Z[J, K; \rho_D]$ can be expressed in terms of a functional integral using standard techniques (see e.g. Refs. [44, 59] and references therein):

$$\begin{aligned} Z[J, K; \rho_D] &= \int [d\varphi_0^+] [d\varphi_0^-] \rho_D [\varphi_0^+, \varphi_0^-] \\ &\times \int_{\varphi^-(t_0, \mathbf{x})=\varphi_0^-(\mathbf{x})}^{\varphi^+(t_0, \mathbf{x})=\varphi_0^+(\mathbf{x})} \mathcal{D}'\varphi^+ \mathcal{D}'\varphi^- \exp \left\{ i \left[S[\varphi^+, \varphi^-] \right. \right. \\ &+ \int_x (\varphi_a^+, \varphi_a^-) \begin{pmatrix} J_a^+ \\ -J_a^- \end{pmatrix} \\ &\left. \left. + \frac{1}{2} \int_{xy} (\varphi_a^+, \varphi_a^-) \begin{pmatrix} K_{ab}^{++} & -K_{ab}^{+-} \\ -K_{ab}^{-+} & K_{ab}^{--} \end{pmatrix} \begin{pmatrix} \varphi_b^+ \\ \varphi_b^- \end{pmatrix} \right] \right\}, \end{aligned} \quad (10)$$

where $\rho_D(\varphi_0^+, \varphi_0^-) = \langle \varphi^+ | \rho_D(t_0) | \varphi^- \rangle$ and the matrix elements are taken with respect to eigenstates of the Heisenberg field operators at initial time, $\Phi_a(t_0, \mathbf{x}) | \varphi^\pm \rangle = \varphi_{0,a}^\pm(\mathbf{x}) | \varphi^\pm \rangle$. In Appendix A, we provide an explicit expression for the initial-state density matrix $\rho_D(\varphi_0^+, \varphi_0^-)$ used later in our numerical calculations. The integral measures are given as $[d\varphi_0^\pm] = \prod_{a,\mathbf{x}} d\varphi_{0,a}^\pm(\mathbf{x})$ and $\mathcal{D}'\varphi^\pm = \prod_{a,x_0>t_0,\mathbf{x}} d\varphi_a^\pm(x_0, \mathbf{x})$, with the prime indicating that the integration over the fields at initial time t_0 is excluded. The superscript '+' ('-') indicates that the sources are taken to be different on the forward (\mathcal{C}^+) and backward (\mathcal{C}^-) branch of the closed time path. Because of the different sources, the corresponding fields on the different branches are labelled accordingly. The minus sign in front of the '-' terms accounts for the reversed time integration. Using this notation the action functional reads

$$\begin{aligned} S[\varphi^+, \varphi^-] &= \frac{1}{2} \int_{xy} (\varphi_a^+, \varphi_a^-) \begin{pmatrix} iG_{0,ab}^{-1} & 0 \\ 0 & -iG_{0,ab}^{-1} \end{pmatrix} \begin{pmatrix} \varphi_b^+ \\ \varphi_b^- \end{pmatrix} \\ &- \frac{g}{8} \int_x (\varphi_a^+ \varphi_a^+ \varphi_b^+ \varphi_b^+ - \varphi_a^- \varphi_a^- \varphi_b^- \varphi_b^-), \end{aligned} \quad (11)$$

which corresponds to the defining action (3) if the time integration is replaced by an integration along the closed time contour \mathcal{C} .

In order to simplify the comparison with the classical statistical field theory below, a standard linear transformation R of the fields is introduced as

$$\begin{pmatrix} \varphi_a \\ \tilde{\varphi}_a \end{pmatrix} \equiv R \begin{pmatrix} \varphi_a^+ \\ \varphi_a^- \end{pmatrix}, \quad (12)$$

where

$$R = \begin{pmatrix} \frac{1}{2} & \frac{1}{2} \\ 1 & -1 \end{pmatrix}, \quad R^{-1} = \begin{pmatrix} 1 & \frac{1}{2} \\ 1 & -\frac{1}{2} \end{pmatrix} \quad (13)$$

such that $\varphi_a = (\varphi_a^+ + \varphi_a^-)/2$ and $\tilde{\varphi}_a = \varphi_a^+ - \varphi_a^-$, or, $\varphi_a^+ = \varphi_a + \tilde{\varphi}_a/2$ and $\varphi_a^- = \varphi_a - \tilde{\varphi}_a/2$, respectively. To avoid a

proliferation of symbols we have used here φ_a , which agrees with the defining field in (3) only for $\varphi_a^+ = \varphi_a^-$. Since this will be the case for expectation values in the absence of sources, where physical observables are obtained, and since there is no danger of confusion in the following we keep this notation.

Correspondingly, we write for the source terms

$$\begin{pmatrix} J_a \\ \tilde{J}_a \end{pmatrix} \equiv R \begin{pmatrix} J_a^+ \\ J_a^- \end{pmatrix}, \quad (14)$$

$$\begin{pmatrix} K_{ab}^F & K_{ab}^R \\ K_{ab}^A & K_{ab}^F \end{pmatrix} \equiv R \begin{pmatrix} K_{ab}^{++} & K_{ab}^{+-} \\ K_{ab}^{-+} & K_{ab}^{--} \end{pmatrix} R^T. \quad (15)$$

Inserting these definitions into the functional integral (10) and using that (14) and (15) can be equivalently written as

$$\begin{pmatrix} \tilde{J}_a \\ J_a \end{pmatrix} \equiv (R^{-1})^T \begin{pmatrix} J_a^+ \\ -J_a^- \end{pmatrix}, \quad (16)$$

$$\begin{pmatrix} K_{ab}^{\tilde{F}} & K_{ab}^A \\ K_{ab}^R & K_{ab}^F \end{pmatrix} \equiv (R^{-1})^T \begin{pmatrix} K_{ab}^{++} & -K_{ab}^{+-} \\ -K_{ab}^{-+} & K_{ab}^{--} \end{pmatrix} R^{-1} \quad (17)$$

one finds:

$$\begin{aligned} Z[J, \tilde{J}, K^F, K^R, K^A, K^{\tilde{F}}; \rho_D] &= \int [d\varphi_0] [d\tilde{\varphi}_0] \rho_D [\varphi_0 + \tilde{\varphi}_0/2, \varphi_0 - \tilde{\varphi}_0/2] \\ &\times \int_{\varphi_0, \tilde{\varphi}_0} \mathcal{D}'\varphi \mathcal{D}'\tilde{\varphi} \exp \left\{ i \left[S[\varphi, \tilde{\varphi}] + \int_x (\varphi_a, \tilde{\varphi}_a) \begin{pmatrix} \tilde{J}_a \\ J_a \end{pmatrix} \right. \right. \\ &\left. \left. + \frac{1}{2} \int_{xy} (\varphi_a, \tilde{\varphi}_a) \begin{pmatrix} K_{ab}^{\tilde{F}} & K_{ab}^A \\ K_{ab}^R & K_{ab}^F \end{pmatrix} \begin{pmatrix} \varphi_b \\ \tilde{\varphi}_b \end{pmatrix} \right] \right\}, \end{aligned} \quad (18)$$

where $S[\varphi, \tilde{\varphi}] = S_0[\varphi, \tilde{\varphi}] + S_{\text{int}}[\varphi, \tilde{\varphi}]$ consists of the action for the free field theory

$$S_0[\varphi, \tilde{\varphi}] = \frac{1}{2} \int_{xy} (\varphi_a, \tilde{\varphi}_a) \begin{pmatrix} 0 & iG_{0,ab}^{-1} \\ iG_{0,ab}^{-1} & 0 \end{pmatrix} \begin{pmatrix} \varphi_b \\ \tilde{\varphi}_b \end{pmatrix} \quad (19)$$

and the interaction part

$$\begin{aligned} S_{\text{int}}[\varphi, \tilde{\varphi}] &= -\frac{g}{2} \int_x \tilde{\varphi}_a(x) \varphi_a(x) \varphi_b(x) \varphi_b(x) \\ &- \frac{g}{8} \int_x \tilde{\varphi}_a(x) \tilde{\varphi}_a(x) \tilde{\varphi}_b(x) \varphi_b(x). \end{aligned} \quad (20)$$

3. Connected one- and two-point functions

From the generating functional for connected correlation functions

$$W = -i \ln Z \quad (21)$$

we define the macroscopic field ϕ_a , and $\tilde{\phi}_a$ by

$$\frac{\delta W}{\delta \tilde{J}_a(x)} = \phi_a(x), \quad \frac{\delta W}{\delta J_a(x)} = \tilde{\phi}_a(x). \quad (22)$$

The connected statistical correlation function $F_{ab}(x, y)$, the retarded/advanced propagators $G_{ab}^{R/A}(x, y)$, and $\tilde{F}_{ab}(x, y)$ are defined by

$$\begin{aligned} \frac{\delta W}{\delta K_{ab}^{\tilde{F}}(x, y)} &= \frac{1}{2} (\phi_a(x)\phi_b(y) + F_{ab}(x, y)) , \\ \frac{\delta W}{\delta K_{ab}^A(x, y)} &= \frac{1}{2} (\phi_a(x)\tilde{\phi}_b(y) - iG_{ab}^R(x, y)) , \\ \frac{\delta W}{\delta K_{ab}^R(x, y)} &= \frac{1}{2} (\tilde{\phi}_a(x)\phi_b(y) - iG_{ab}^A(x, y)) , \\ \frac{\delta W}{\delta K_{ab}^F(x, y)} &= \frac{1}{2} (\tilde{\phi}_a(x)\tilde{\phi}_b(y) + \tilde{F}_{ab}(x, y)) . \end{aligned} \quad (23)$$

For vanishing sources the field $\tilde{\phi} \equiv 0$ and the propagator $\tilde{F} \equiv 0$ [59]. Moreover, the retarded and advanced correlators $G^R(x, y)$ and $G^A(y, x)$ vanish for $x_0 < y_0$. (See also the discussion in Sect. II B 3.) In the absence of sources, these two-point functions are related then through the transformation (13),

$$\begin{pmatrix} F_{ab} & -iG_{ab}^R \\ -iG_{ab}^A & 0 \end{pmatrix} = R \begin{pmatrix} G_{ab}^{++} & G_{ab}^{+-} \\ G_{ab}^{-+} & G_{ab}^{--} \end{pmatrix} R^T, \quad (24)$$

to the time-ordered correlation functions written in the ‘ \pm ’ basis. The inverse of the two-point function matrix (24) reads

$$\begin{pmatrix} 0 & i(G^A)_{ab}^{-1} \\ i(G^R)_{ab}^{-1} & X_{ab}^{-1} \end{pmatrix}, \quad (25)$$

where

$$\begin{aligned} X_{ab}^{-1}(x, y) &\equiv \int_{zw} (G^R)_{ac}^{-1}(x, z) F_{cd}(z, w) (G^A)_{db}^{-1}(w, y) \\ &\equiv [(G^R)^{-1} \cdot F \cdot (G^A)^{-1}]_{ab}(x, y). \end{aligned} \quad (26)$$

The last equation introduces a compact matrix notation that will be employed below.

4. 2PI effective action

The 2PI effective action is obtained as the Legendre transform

$$\begin{aligned} \Gamma &= W - \int_x (\phi_a(x)\tilde{J}_a(x) + \tilde{\phi}_a(x)J_a(x)) \\ &\quad - \frac{1}{2} \int_{xy} \left\{ K_{ab}^{\tilde{F}}(x, y) (\phi_a(x)\phi_b(y) + F_{ab}(x, y)) \right. \\ &\quad + K_{ab}^A(x, y) (\phi_a(x)\tilde{\phi}_b(y) - iG_{ab}^R(x, y)) \\ &\quad + K_{ab}^R(x, y) (\tilde{\phi}_a(x)\phi_b(y) - iG_{ab}^A(x, y)) \\ &\quad \left. + K_{ab}^F(x, y) (\tilde{\phi}_a(x)\tilde{\phi}_b(y) + \tilde{F}_{ab}(x, y)) \right\}. \end{aligned} \quad (27)$$

This corresponds to the 2PI effective action originally discussed in Refs. [31, 32, 33], however, written in terms of the

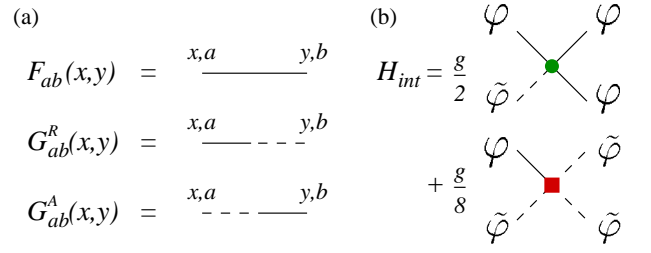


FIG. 1: (color online) (a) Diagrammatic representation of the correlators in the φ - $\tilde{\varphi}$ basis. A full line indicates the 1- or φ -component, a broken line the 2- or $\tilde{\varphi}$ -component. $F_{ab}(x, y)$ is the statistical correlation function, $G_{ab}^R(x, y) = \rho_{ab}(x, y)\theta(x_0 - y_0)$ and $G_{ab}^A(x, y) = -\rho_{ab}(x, y)\theta(y_0 - x_0)$ the retarded and advanced Green's functions, respectively. Their representation in terms of the real-valued spectral correlation function $\rho_{ab}(x, y)$ exposes the θ -functions which imply the respective time ordering in x_0, y_0 . (b) Diagrammatic expansion of the quantum vertex term entering the action (3). The classical action (53) is lacking the second contribution (red square).

rotated variables. From (27) one observes the equations of motion for the fields

$$\begin{aligned} \frac{\delta \Gamma}{\delta \phi_a(x)} &= -\tilde{J}_a(x) - \int_y \left(K_{ab}^{\tilde{F}}(x, y)\phi_b(y) \right. \\ &\quad \left. + \frac{1}{2}K_{ab}^A(x, y)\tilde{\phi}_b(y) + \frac{1}{2}\tilde{\phi}_b(y)K_{ba}^R(y, x) \right), \end{aligned} \quad (28)$$

$$\begin{aligned} \frac{\delta \Gamma}{\delta \tilde{\phi}_a(x)} &= -J_a(x) - \int_y \left(K_{ab}^F(x, y)\tilde{\phi}_b(y) \right. \\ &\quad \left. + \frac{1}{2}K_{ab}^R(x, y)\phi_b(y) + \frac{1}{2}\phi_b(y)K_{ba}^A(y, x) \right), \end{aligned} \quad (29)$$

as well as for the two-point functions

$$\frac{\delta \Gamma}{\delta F_{ab}(x, y)} = -\frac{1}{2}K_{ab}^{\tilde{F}}(x, y), \quad (30)$$

$$i\frac{\delta \Gamma}{\delta G_{ab}^R(x, y)} = -\frac{1}{2}K_{ab}^A(x, y), \quad (31)$$

$$i\frac{\delta \Gamma}{\delta G_{ab}^A(x, y)} = -\frac{1}{2}K_{ab}^R(x, y), \quad (32)$$

$$\frac{\delta \Gamma}{\delta \tilde{F}_{ab}(x, y)} = -\frac{1}{2}K_{ab}^F(x, y). \quad (33)$$

The diagrammatic calculation of the 2PI effective action involves all closed two-particle irreducible Feynman graphs with lines associated to the full two-point correlators [31, 32, 33]. This is illustrated in Fig. 1 for vanishing macroscopic field ϕ and in the absence of external sources.

In the presence of a non-vanishing field value, $\phi \neq 0$, the interaction vertices are obtained from (20) by shifting in $S[\varphi, \tilde{\varphi}]$ the field $\varphi \rightarrow \phi + \varphi$, and collecting all cubic and

quartic terms in the fluctuating fields φ and $\tilde{\varphi}$, i.e.

$$\begin{aligned} S_{\text{int}}[\varphi, \tilde{\varphi}; \phi] &= -\frac{g}{2} \int_x \tilde{\varphi}_a(x) \varphi_a(x) \varphi_b(x) \varphi_b(x) \\ &\quad -\frac{g}{8} \int_x \tilde{\varphi}_a(x) \tilde{\varphi}_a(x) \tilde{\varphi}_b(x) \varphi_b(x) \\ &\quad -g \int_x \tilde{\varphi}_a(x) \varphi_a(x) \varphi_b(x) \phi_b(x) \\ &\quad -\frac{g}{2} \int_x \tilde{\varphi}_a(x) \phi_a(x) \varphi_b(x) \varphi_b(x) \\ &\quad -\frac{g}{8} \int_x \tilde{\varphi}_a(x) \tilde{\varphi}_a(x) \tilde{\varphi}_b(x) \phi_b(x). \end{aligned} \quad (34)$$

The quadratic terms in the fluctuating fields are taken into account in the classical inverse propagator (4) by the replacement

$$H_{1B} \delta_{ab} \rightarrow \left[H_{1B} + \frac{g}{2} \phi_c(x) \phi_c(x) \right] \delta_{ab} + g \phi_a(x) \phi_b(x). \quad (35)$$

In the free part of the action (19), and in the dynamic equations derived below, this corresponds to a field dependent $iG_0^{-1}(x, y; \phi)$, while the general form of the equations remains unchanged [74]. We note that linear terms in the fluctuating fields ensure cancellation of possible tadpole contributions, which therefore do not need to be considered explicitly.

5. Exact evolution equations

For vanishing sources, the exact inverse two-point function (25) can then be written as [31, 32, 33]

$$\begin{aligned} &\begin{pmatrix} 0 & i(G^A)^{-1} \\ i(G^R)^{-1} & X_{ab}^{-1} \end{pmatrix} \\ &= \begin{pmatrix} 0 & G_{0,ab}^{-1} \\ G_{0,ab}^{-1} & 0 \end{pmatrix} - \begin{pmatrix} 0 & -i\Sigma_{ab}^A \\ -i\Sigma_{ab}^R & \Sigma_{ab}^F \end{pmatrix}, \end{aligned} \quad (36)$$

where X^{-1} is defined in Eq. (26) and the retarded, advanced and statistical self-energies are related through the transformation (13),

$$\begin{pmatrix} 0 & -i\Sigma_{ab}^A \\ -i\Sigma_{ab}^R & \Sigma_{ab}^F \end{pmatrix} = (R^{-1})^T \begin{pmatrix} \Sigma_{ab}^{++} & -\Sigma_{ab}^{+-} \\ -\Sigma_{ab}^{-+} & \Sigma_{ab}^{--} \end{pmatrix} R^{-1}, \quad (37)$$

to the self-energies written in the ‘ \pm ’ basis. To the retarded/advanced self-energy $\Sigma^{R/A}$ and the statistical self-energy Σ^F contribute only graphs with propagator lines associated to $G^{R,A}$ and F , which can be obtained from closed two-particle irreducible graphs by opening one propagator line [31, 32, 33].

To convert Eq. (36) for the inverse propagator into an equation, which is more suitable for initial value problems, we convolute with the propagator matrix (24) from the right and with the classical propagator from the left. This yields the Schwinger-Dyson equations for the retarded/advanced propagator in the absence of sources,

$$G^{R/A} = G_0^{R/A} - G_0^{R/A} \cdot \Sigma^{R/A} \cdot G^{R/A}, \quad (38)$$

and the statistical propagator,

$$F = F_0 - F_0 \cdot \Sigma^A \cdot G^A - G_0^R \cdot [\Sigma^R \cdot F + \Sigma^F \cdot G^A], \quad (39)$$

where we have used the compact notation introduced in Eq. (26). For the spectral function,

$$\rho_{ab}(x, y) = G_{ab}^R(x, y) - G_{ab}^A(x, y), \quad (40)$$

the Schwinger-Dyson equation follows from Eqs. (40) and (38) as

$$\rho = \rho_0 - G_0^R \cdot \Sigma^R \cdot G^R + G_0^A \cdot \Sigma^A \cdot G^A. \quad (41)$$

Acting on Eqs. (39) and (41) with G_0^{-1} from the left brings these equations in a form which is more suitable for initial-value problems. For this we write

$$\Sigma_{ab}^R(x, y; \phi) = \Sigma_{ab}^{(0)}(x) \delta(x - y) + \theta(x_0 - y_0) \Sigma_{ab}^\rho(x, y; \phi), \quad (42)$$

where we introduce the spectral part of the self-energy

$$\Sigma_{ab}^\rho(x, y; \phi) = \Sigma_{ab}^R(x, y; \phi) - \Sigma_{ab}^A(x, y; \phi). \quad (43)$$

Using that F_0 and ρ_0 satisfy the homogeneous field equations

$$\begin{aligned} \int_z G_{0,ac}^{-1}(x, z) F_{0,cb}(z, y) &= 0, \\ \int_z G_{0,ac}^{-1}(x, z) \rho_{0,cb}(z, y) &= 0, \end{aligned} \quad (44)$$

and taking into account all θ -functions one obtains the dynamic equations for the two-point correlation functions F and ρ [36, 45, 70]:

$$\begin{aligned} &[i\sigma_{ac}^2 \partial_{x_0} + M_{ac}(x)] F_{cb}(x, y) \\ &= - \int_{t_0}^{x_0} dz \Sigma_{ac}^\rho(x, z; \phi) F_{cb}(z, y) \\ &\quad + \int_{t_0}^{y_0} dz \Sigma_{ac}^F(x, z; \phi) \rho_{cb}(z, y), \\ &[i\sigma_{ac}^2 \partial_{x_0} + M_{ac}(x)] \rho_{cb}(x, y) \\ &= - \int_{y_0}^{x_0} dz \Sigma_{ac}^\rho(x, z; \phi) \rho_{cb}(z, y), \end{aligned} \quad (45)$$

where we employ the notation

$$\int_{t_0}^{x_0} dz \equiv \int_{t_0}^{x_0} dz_0 \int d^d z. \quad (46)$$

Here

$$\begin{aligned} M_{ab}(x) &= \delta_{ab} \left[H_{1B}(x) + \frac{g}{2} (\phi_c(x) \phi_c(x) + F_{cc}(x, x)) \right] \\ &\quad + g (\phi_a(x) \phi_b(x) + F_{ab}(x, x)) \end{aligned} \quad (47)$$

is the mean-field energy matrix which includes the field-dependent terms of the classical inverse propagator $iG_{0,ab}^{-1}(\phi)$

defined in Eqs. (4) with (35), and the local part of the self-energy,

$$\Sigma_{ab}^{(0)}(x) = \frac{g}{2}\delta_{ab}F_{cc}(x, x) + gF_{ab}(x, x), \quad (48)$$

as defined in Eq. (43). We note that the spectral function at initial time is characterized by the commutator (8), with

$$\rho_{ab}(x, y)|_{x_0=y_0} = -i\sigma_{ab}^2\delta(\mathbf{x} - \mathbf{y}), \quad (49)$$

for the non-relativistic theory.

The dynamic equation for the mean field $\phi_a(x)$ is obtained from Eq. (29) with $\tilde{\phi}_a(x) \equiv 0$ in the absence of sources. It reads [35, 36]:

$$\begin{aligned} & \left(-i\sigma_{ab}^2\partial_{x_0} - gF_{ab}(x, x) \right) \phi_b(x) - \left(H_{1B}(x) \right. \\ & \left. + \frac{g}{2}[\phi_c(x)\phi_c(x) + F_{cc}(x, x)] \right) \phi_a(x) = \frac{\delta\Gamma_2}{\delta\phi_a(x)}, \end{aligned} \quad (50)$$

where the functional derivative is taken for fixed two-point functions and Γ_2 contains all closed 2PI graphs [31, 32, 33]. In Sec. II C we will employ an expansion in the number of field components to next-to-leading order to approximately describe the dynamics, for which one obtains the compact expression [35]

$$\frac{\delta\Gamma_2}{\delta\phi_a(x)} = \int_{t_0}^{x_0} dy \Sigma_{ab}^\rho(x, y; \phi \equiv 0) \phi_b(y). \quad (51)$$

B. Classical statistical dynamics

1. Classical equation of motion

The classical field equation of motion can be derived from the defining action (3). In the basis (12) the same equation of motion for the field $\varphi_a(x)$ is obtained from the action with (19) and (20) by

$$\frac{\delta S[\varphi, \tilde{\varphi}]}{\delta \tilde{\varphi}} \Big|_{\varphi=\varphi^{\text{cl}}, \tilde{\varphi}=0} = \frac{\delta S^{\text{cl}}[\varphi, \tilde{\varphi}]}{\delta \tilde{\varphi}} \Big|_{\varphi=\varphi^{\text{cl}}} = 0, \quad (52)$$

as a consequence of setting $\tilde{\varphi} = 0$. For the first identity in (52) we have defined $S^{\text{cl}}[\varphi, \tilde{\varphi}] \equiv S_0[\varphi, \tilde{\varphi}] + S_{\text{int}}^{\text{cl}}[\varphi, \tilde{\varphi}]$ as that part of $S[\varphi, \tilde{\varphi}]$ which is linear in $\tilde{\varphi}$. As a consequence, the non-interacting part $S_0[\varphi, \tilde{\varphi}]$ agrees with the respective expression appearing for the quantum theory (19). The interaction part of $S^{\text{cl}}[\varphi, \tilde{\varphi}]$, however, differs from (20) in that it contains fewer vertices:

$$S_{\text{int}}^{\text{cl}}[\varphi, \tilde{\varphi}] = -\frac{g}{2} \int_x \tilde{\varphi}_a(x)\varphi_a(x)\varphi_b(x)\varphi_b(x). \quad (53)$$

This is illustrated in Fig. 1b. The absence of vertices beyond those which are linear in $\tilde{\varphi}$ turns out to be the crucial difference between a classical and a quantum statistical field theory as is discussed in the following.

2. Classical statistical generating functional

We will construct the generating functional for the classical statistical field theory, $Z^{\text{cl}}[J, K; W]$ for given probability functional W for the fields at initial time, similar to the expression (18) for the quantum theory. For this, we rewrite the equation of motion (52) as a δ -constraint in a functional integral using the Fourier transform representation

$$\begin{aligned} \delta \left[\frac{\delta S^{\text{cl}}[\varphi, \tilde{\varphi}]}{\delta \tilde{\varphi}} \right] &= \int \mathcal{D}\tilde{\varphi} \exp \left\{ i \int_x \frac{\delta S^{\text{cl}}[\varphi, \tilde{\varphi}]}{\delta \tilde{\varphi}_a(x)} \tilde{\varphi}_a(x) \right\} \\ &= \int \mathcal{D}\tilde{\varphi} \exp \left\{ i S^{\text{cl}}[\varphi, \tilde{\varphi}] + i \int_{\mathbf{x}} \pi_{0,a}(\mathbf{x}) \tilde{\varphi}_{0,a}(\mathbf{x}) \right\}. \end{aligned} \quad (54)$$

For the last equality, the second term in the exponent subtracts the boundary term at the initial time t_0 , which follows from partial integration. We emphasize that we have to take into account this boundary term since t_0 will be taken to be finite for the nonequilibrium initial-value problems considered. Note that in the path integral (18), the action $S[\varphi, \tilde{\varphi}]$ is implied not to depend on boundary terms at initial time t_0 . (As a consequence, the term $i \int_{\mathbf{x}} \pi_{0,a}(\mathbf{x}) \tilde{\varphi}_{0,a}(\mathbf{x})$ appears in Eq. (54) and not half of it.) Here $\pi_{0,a}(\mathbf{x}) = \pi_a(x_0 = t_0, \mathbf{x})$ is the initial canonical momentum, with $\pi_a(x) = i\sigma_{ab}^2\varphi_b(x)$ for the non-relativistic theory as in Eq. (6). We note that Eq. (54) remains valid also for a relativistic theory, where $\pi_{0,a}(\mathbf{x})$ denotes the time derivative of the field at time t_0 .

It should be stressed that the Fourier transform expression (54) could not be achieved with $S^{\text{cl}}[\varphi, \tilde{\varphi}]$ replaced by $S[\varphi, \tilde{\varphi}]$ since the latter is not linear in $\tilde{\varphi}$. For the non-interacting theory, however, $S_0^{\text{cl}}[\varphi, \tilde{\varphi}] = S_0[\varphi, \tilde{\varphi}]$ holds, and we will recover the fact that the free classical and quantum theories are governed by the same dynamics for same initial conditions. The same fact holds true for all Gaussian (leading-order large- \mathcal{N} or Hartree-type) approximations. Therefore, it is crucial for a quantum classical comparison that we go beyond and consider the next-to-leading order corrections as we do in Sect. II A 4 below.

Any functional $f[\varphi^{\text{cl}}]$ of the classical field φ^{cl} , being a solution of the classical equation of motion (52), can be written as

$$\begin{aligned} f[\varphi^{\text{cl}}] &= \int_{\varphi_0=\varphi_0^{\text{cl}}} \mathcal{D}'\varphi f[\varphi] \delta[\varphi^{\text{cl}} - \varphi] \\ &= \int_{\varphi_0=\varphi_0^{\text{cl}}} \mathcal{D}'\varphi f[\varphi] \delta \left[\frac{\delta S^{\text{cl}}[\varphi, \tilde{\varphi}]}{\delta \tilde{\varphi}} \right] \mathcal{J}[\varphi] \\ &= \int_{\varphi_0=\varphi_0^{\text{cl}}} \mathcal{D}'\varphi \mathcal{D}\tilde{\varphi} f[\varphi] \\ &\quad \times \exp \left\{ i S^{\text{cl}}[\varphi, \tilde{\varphi}] + i \int_{\mathbf{x}} \pi_{0,a} \tilde{\varphi}_{0,a} \right\} \mathcal{J}[\varphi], \end{aligned} \quad (55)$$

where the Jacobian reads

$$\mathcal{J}[\varphi] = \left| \det \left(\frac{\delta^2 S^{\text{cl}}[\varphi, \tilde{\varphi}]}{\delta\varphi\delta\tilde{\varphi}} \right) \right|. \quad (56)$$

Here the Jacobian plays the role of an irrelevant normalization constant, which has been discussed in detail in Ref. [66] and references therein.

Classical correlation functions are obtained as phase-space averages over trajectories given by solutions of the classical field equation (52). Such averages, for an arbitrary functional of the field, are defined as

$$\langle f[\varphi_a] \rangle_{\text{cl}} = \int [d\varphi_0^{\text{cl}}][d\pi_0^{\text{cl}}] W[\varphi_0^{\text{cl}}, \pi_0^{\text{cl}}] f[\varphi_a^{\text{cl}}]. \quad (57)$$

Here $W[\varphi_0^{\text{cl}}, \pi_0^{\text{cl}}]$ denotes the normalized phase-space probability functional at initial time (and is not to be confused with the generating functional (21)). In Appendix A we provide an explicit expression for $W[\varphi_0^{\text{cl}}, \pi_0^{\text{cl}}]$, a functional of four fields which is symmetric under the exchange of $\pi_{0,a}^{\text{cl}}$ and $i\sigma_{ab}^2\varphi_{0,b}^{\text{cl}}$ for $a = 1, 2$, since the canonical momentum (6) is proportional to the field itself. The measure indicates integration over the classical phase-space. The theory may be defined on a spatial lattice to regulate the Rayleigh-Jeans divergence of classical statistical field theory.

Using Eqs. (55) and (57), we can now write down a generating functional for classical correlation functions in the form:

$$\begin{aligned} Z^{\text{cl}}[J, \tilde{J}, K^F, K^R, K^A, K^{\tilde{F}}; W] &= \int [d\varphi_0^{\text{cl}}][d\pi_0^{\text{cl}}] W[\varphi_0^{\text{cl}}, \pi_0^{\text{cl}}] \\ &\times \int_{\varphi_0=\varphi_0^{\text{cl}}, \pi_0=\pi_0^{\text{cl}}} \mathcal{D}'\varphi \mathcal{D}\tilde{\varphi} \exp \left\{ i \left[S^{\text{cl}}[\varphi, \tilde{\varphi}] + \int_{\mathbf{x}} \pi_{0,a} \tilde{\varphi}_{0,a} \right. \right. \\ &+ \int_x (\varphi_a, \tilde{\varphi}_a) \begin{pmatrix} \tilde{J}_a \\ J_a \end{pmatrix} \\ &\left. \left. + \frac{1}{2} \int_{xy} (\varphi_a, \tilde{\varphi}_a) \begin{pmatrix} K_{ab}^{\tilde{F}} & K_{ab}^A \\ K_{ab}^R & K_{ab}^F \end{pmatrix} \begin{pmatrix} \varphi_b \\ \tilde{\varphi}_b \end{pmatrix} \right] \right\} \mathcal{J}[\varphi], \end{aligned} \quad (58)$$

where $S^{\text{cl}}[\varphi, \tilde{\varphi}] = S_0[\varphi, \tilde{\varphi}] + S_{\text{int}}^{\text{cl}}[\varphi, \tilde{\varphi}]$ as defined in Eqs. (19) and (53), and where the relation (6) between the field and the canonical momentum is implied.

Comparing with the quantum generating functional in Eq. (18), and using that the Jacobian $\mathcal{J}[\varphi]$ plays the role of an irrelevant normalization constant, we find that the classical functional (58) takes the same Lagrangian form, with initial conditions given by a density matrix ρ_D which is characterized by the Fourier transform of the phase-space probability distribution $W[\varphi_0, \pi_0]$:

$$\begin{aligned} \rho_D[\varphi_0 + \tilde{\varphi}_0/2, \varphi_0 - \tilde{\varphi}_0/2] \\ = \int [d\pi_0] W[\varphi_0, \pi_0] \exp \left\{ i \int_{\mathbf{x}} \pi_{0,a} \tilde{\varphi}_{0,a} \right\}. \end{aligned} \quad (59)$$

In summary, the generating functionals for correlation functions are very similar in the quantum and the classical statistical theory. The crucial difference is that the quantum theory is characterized by more vertices. As a consequence, we can follow the very same steps as in Sect. II A to construct the classical statistical 2PI effective action and to derive the time evolution equations from it.

Similar to the discussion for the quantum theory above, for $\phi \neq 0$ the interaction vertices for the classical statistical theory are obtained by shifting in $S^{\text{cl}}[\varphi, \tilde{\varphi}]$ the field $\varphi \rightarrow \phi + \varphi$, and collecting all cubic and quartic terms in the fluctuating fields, i.e.

$$\begin{aligned} S_{\text{int}}^{\text{cl}}[\varphi, \tilde{\varphi}; \phi] &= -\frac{g}{2} \int_x \tilde{\varphi}_a(x) \varphi_a(x) \varphi_b(x) \varphi_b(x) \\ &- g \int_x \tilde{\varphi}_a(x) \varphi_a(x) \varphi_b(x) \phi_b(x) \\ &- \frac{g}{2} \int_x \tilde{\varphi}_a(x) \phi_a(x) \varphi_b(x) \varphi_b(x). \end{aligned} \quad (60)$$

This can be compared to the respective expression for the quantum theory, Eq. (34).

3. Correlation functions

Comparing quantum and classical statistical dynamics amounts to comparing the time evolution of classical statistical n -point functions with that of the respective quantum ones. The classical functions are obtained as phase-space averages (57) over trajectories given by solutions of the classical field equation (52). As an example, the macroscopic or average classical field is given by

$$\phi_a^{\text{cl}}(x) = \langle \varphi_a(x) \rangle_{\text{cl}} = \int [d\varphi_0^{\text{cl}}][d\pi_0^{\text{cl}}] W[\varphi_0^{\text{cl}}, \pi_0^{\text{cl}}] \varphi_a^{\text{cl}}(x). \quad (61)$$

This is equivalent to the field average obtained from the generating functional (58) by functional differentiation with respect to $J_a(x)$. Similarly, also $\tilde{\phi}_a^{\text{cl}}(x)$ can be obtained by functional differentiation with respect to $J_a(x)$ in the same way as described in Sect. II A 3 if the quantum generating functional in Eq. (21) is replaced by its classical counterpart defined in Eq. (58). Moreover, as for the quantum case, $\phi_a(x) \equiv 0$ for vanishing sources. This can be directly seen by taking the functional derivative of Z^{cl} with respect to $J_a(x)$, setting all sources to zero except $J_a(x)$, and performing all steps backward in Eqs. (58) and (55). This is possible as the remaining source term is linear in $\tilde{\varphi}$. Using the same reasoning one finds that also the two-point correlation function $\tilde{F}_{ab}(x, y)$, which is defined as in Eq. (23) as a functional derivative of $W^{\text{cl}} = -i \ln Z^{\text{cl}}$ with respect to K^F , vanishes identically in the absence of sources.

Similarly, defining the connected classical statistical propagator $F_{ab}^{\text{cl}}(x, y)$ according to Eq. (23) results in

$$\begin{aligned} F_{ab}^{\text{cl}}(x, y) + \phi_a^{\text{cl}}(x) \phi_b^{\text{cl}}(y) &= \langle \varphi_a(x) \varphi_b(y) \rangle_{\text{cl}} \\ &= \int [d\varphi_0^{\text{cl}}][d\pi_0^{\text{cl}}] W[\varphi_0^{\text{cl}}, \pi_0^{\text{cl}}] \varphi_a^{\text{cl}}(x) \varphi_b^{\text{cl}}(y). \end{aligned} \quad (62)$$

The classical equivalent of the quantum spectral function $\rho_{ab}^{\text{cl}}(x, y)$ is obtained as follows: Taking the functional deriva-

tives according to Eq. (23) leads, with Eq. (40), to

$$\begin{aligned} \rho_{ab}(x, y) &= \int [d\varphi_0^{\text{cl}}][d\pi_0^{\text{cl}}] W[\varphi_0^{\text{cl}}, \pi_0^{\text{cl}}] \\ &\times i \int_{\varphi_0=\varphi_0^{\text{cl}}, \pi_0=\pi_0^{\text{cl}}} \mathcal{D}'\varphi \mathcal{D}\tilde{\varphi} [\varphi_a(x)\tilde{\varphi}_b(y) - \tilde{\varphi}_a(x)\varphi_b(y)] \\ &\times \exp \left\{ i \left[S^{\text{cl}}[\varphi, \tilde{\varphi}] + \int_{\mathbf{x}} \pi_{0,a} \tilde{\varphi}_{0,a} \right] \right\} \mathcal{J}[\varphi]. \end{aligned} \quad (63)$$

If $x_0 < y_0$ the expectation value of $\varphi_a(x)\tilde{\varphi}_b(y)$ vanishes following the same reasoning as for the field $\tilde{\phi}^{\text{cl}}$, in accordance with the fact that this term corresponds to the retarded propagator $G^{\text{R}}(x, y)$. Analogously, if $x_0 > y_0$, the advanced propagator, i.e. the average of $\tilde{\varphi}_a(x)\varphi_b(y)$, vanishes.

We consider the case that $x_0 = t_0$. If $y_0 > x_0$, one obtains from Eq. (63) and the definition (6) of the canonical field momentum:

$$\begin{aligned} &\int [d\varphi_0^{\text{cl}}][d\pi_0^{\text{cl}}] W[\varphi_0^{\text{cl}}, \pi_0^{\text{cl}}] \frac{\delta}{\delta\pi_{0,a}^{\text{cl}}(\mathbf{x})} \int_{\varphi_0=\varphi_0^{\text{cl}}, \pi_0=\pi_0^{\text{cl}}} \mathcal{D}'\varphi \mathcal{D}\tilde{\varphi} \varphi_b(y) \\ &\times \exp \left\{ i \left[S^{\text{cl}}[\varphi, \tilde{\varphi}] + \int_{\mathbf{x}} \pi_{0,a} \tilde{\varphi}_{0,a} \right] \right\} \mathcal{J}[\varphi] \\ &= - \int [d\varphi_0^{\text{cl}}][d\pi_0^{\text{cl}}] W[\varphi_0^{\text{cl}}, \pi_0^{\text{cl}}] \frac{\delta\varphi_b^{\text{cl}}(y)}{\delta\pi_{0,a}^{\text{cl}}(\mathbf{x})} \\ &= - \int [d\varphi_0^{\text{cl}}][d\pi_0^{\text{cl}}] W[\varphi_0^{\text{cl}}, \pi_0^{\text{cl}}] \int_{\mathbf{z}} \frac{\delta\varphi_a^{\text{cl}}(t_0, \mathbf{x})}{\delta\varphi_{0,c}^{\text{cl}}(\mathbf{z})} \frac{\delta\varphi_b^{\text{cl}}(y)}{\delta\pi_{0,c}^{\text{cl}}(\mathbf{z})}. \end{aligned} \quad (64)$$

Extending this procedure to $t_0 = y_0 \leq x_0$ one recovers the well-known fact that the classical spectral function is obtained by replacing $-i$ times the commutator with the Poisson bracket:

$$\rho_{ab}^{\text{cl}}(x, y) = -\langle \{\varphi_a(x), \varphi_b(y)\}_{\text{PB}} \rangle_{\text{cl}}. \quad (65)$$

The Poisson bracket with respect to the initial fields is

$$\begin{aligned} \{\varphi_a(x), \varphi_b(y)\}_{\text{PB}} &= \int_{\mathbf{z}} \left[\frac{\delta\varphi_a(x)}{\delta\varphi_{0,c}(\mathbf{z})} \frac{\delta\varphi_b(y)}{\delta\pi_{0,c}(\mathbf{z})} \right. \\ &\quad \left. - \frac{\delta\varphi_a(x)}{\delta\pi_{0,c}(\mathbf{z})} \frac{\delta\varphi_b(y)}{\delta\varphi_{0,c}(\mathbf{z})} \right] \end{aligned} \quad (66)$$

(Summation over c). Note that, in order to arrive at Eq. (65), we used that the Poisson brackets are invariant under the classical time evolution of the fields and therefore valid for any times x_0, y_0 .

As a consequence, one finds the equal-time relations for the classical spectral function: $\rho_{ab}^{\text{cl}}(x, y)|_{x_0=y_0} = -i\sigma_{ab}^2\delta(\mathbf{x} - \mathbf{y})$. Note that they are in complete correspondence with the respective quantum relations in Eq. (49). Equivalently, the free spectral function $\rho_{0,cb}^{\text{cl}}(x, y)$ and statistical function $F_{0,cb}^{\text{cl}}(x, y)$ are solutions of the homogeneous equations corresponding to Eq. (44), with initial conditions determined for ρ_0^{cl} by the equal-time canonical relations, and for F_0^{cl} by the

initial probability functional $W[\varphi_0, \pi_0]$. Also for the classical statistical theory Eqs. (50) and (45) are the exact equations for the field ϕ and the correlation functions F and ρ , respectively. There is a difference between the classical and quantum equations of motion only in the self-energy contributions corresponding to Σ^F and Σ^ρ . This difference arises from the different properties of the interaction part of the quantum and classical actions (20) and (53), respectively. We discuss this difference for the non-perturbative 2PI $1/\mathcal{N}$ expansion to next-to-leading order in the following subsection.

Summarizing, one finds when comparing classical statistical and quantum many-body dynamics that the generating functionals for correlation functions are very similar in the classical and the quantum theory. However, the quantum theory is characterized by more vertices. As a consequence, the same techniques can be used to derive time evolution equations of classical correlation functions that are employed in quantum field theory. Eventually, in the basis corresponding to the fields φ and $\tilde{\varphi}$, the classical dynamic equations have the same form as their quantum analogues but are lacking certain terms due to the reduced number of vertices.

C. Quantum versus classical statistical evolution

The classical statistical generating functional (58) exhibits an important reparametrization property: If the fluctuating fields are rescaled according to

$$\begin{aligned} \varphi_a(x) &\rightarrow \varphi'_a(x) = \sqrt{g}\varphi_a(x), \\ \tilde{\varphi}_a(x) &\rightarrow \tilde{\varphi}'_a(x) = (1/\sqrt{g})\tilde{\varphi}_a(x) \end{aligned} \quad (67)$$

then the coupling g drops out of $S^{\text{cl}}[\varphi, \tilde{\varphi}] = S_0[\varphi, \tilde{\varphi}] + S_{\text{int}}^{\text{cl}}[\varphi, \tilde{\varphi}]$ defined in Eqs. (19) and (53). The free part $S_0[\varphi, \tilde{\varphi}]$ remains unchanged and the interaction part becomes

$$S_{\text{int}}^{\text{cl}}[\varphi', \tilde{\varphi}'] = -\frac{1}{2} \int_x \tilde{\varphi}'_a(x)\varphi'_a(x)\varphi'_b(x)\varphi'_b(x). \quad (68)$$

Moreover, the functional measure in Eq. (58) is invariant under the rescaling (67), and the sources can be redefined accordingly. Therefore, the classical statistical generating functional becomes independent of g , except for the coupling dependence entering the probability distribution fixing the initial conditions. Accordingly, the coupling does not enter the classical dynamic equations for correlation functions. All the g -dependence enters the initial conditions which are required to solve the dynamic equations.

In contrast to the classical case, this reparametrization property is absent for the quantum theory: After the rescaling (67) one is left with $S[\varphi', \tilde{\varphi}']$ whose coupling dependence is given by the interaction part

$$\begin{aligned} S_{\text{int}}[\varphi', \tilde{\varphi}'] &= -\frac{1}{2} \int_x \tilde{\varphi}'_a(x)\varphi'_a(x)\varphi'_b(x)\varphi'_b(x) \\ &\quad -\frac{g^2}{8} \int_x \tilde{\varphi}'_a(x)\tilde{\varphi}'_a(x)\tilde{\varphi}'_b(x)\varphi'_b(x), \end{aligned} \quad (69)$$

according to Eq. (20). Comparing to (68) one observes that the ‘quantum’ vertex, which is absent in the classical statistical theory, encodes all the g -dependence of the dynamics.

The comparison of quantum versus classical dynamics becomes particularly transparent using the above rescaling. The rescaled macroscopic field and statistical correlation function are given by

$$\phi'_a(x) = \sqrt{g}\phi_a(x), \quad F'_{ab}(x, y) = gF_{ab}(x, y), \quad (70)$$

while the spectral function $\rho_{ab}(x, y)$ remains unchanged according to Eqs. (23) and (40). Similarly, we define for the statistical self-energy entering the dynamic equations (45)

$$\Sigma_{ab}^{F'}(x, y) = g\Sigma_{ab}^F(x, y). \quad (71)$$

1. Quantum versus classical statistical self-energy

To identify the precise difference between the quantum and the classical time evolution, details about the self-energies are required. In the following we will employ the 2PI $1/\mathcal{N}$ expansion to next-to-leading order [34, 35]. This is a nonperturbative expansion in powers of the inverse number of field components \mathcal{N} which, in the context of a non-relativistic Bose gas, is $\mathcal{N} = 2$ as discussed in detail in Ref. [36]. We quote the result for the self-energies for $\mathcal{N} = 2$ [34, 35], which for the rescaled variables (70) and (71) read:

$$\begin{aligned} \Sigma_{ab}^{F'}(x, y) &= -\left\{ I'_F(x, y)\phi'_a(x)\phi'_b(y) \right. \\ &\quad + [I'_F(x, y) + P'_F(x, y)]F'_{ab}(x, y) \\ &\quad \left. - \frac{g^2}{4} [I_\rho(x, y) + P_\rho(x, y)]\rho_{ab}(x, y) \right\}, \\ \Sigma_{ab}^\rho(x, y) &= -\left\{ I_\rho(x, y)\phi'_a(x)\phi'_b(y) \right. \\ &\quad + [I_\rho(x, y) + P_\rho(x, y)]F'_{ab}(x, y) \\ &\quad \left. + [I'_F(x, y) + P'_F(x, y)]\rho_{ab}(x, y) \right\}. \end{aligned} \quad (72)$$

The functions I'_F and I_ρ satisfy

$$\begin{aligned} I'_F(x, y) &= -\Pi'_F(x, y) \\ &\quad + \int_{t_0}^{x_0} dz I_\rho(x, z)\Pi'_F(z, y) \\ &\quad - \int_{t_0}^{y_0} dz I'_F(x, z)\Pi_\rho(z, y), \\ I_\rho(x, y) &= -\Pi_\rho(x, y) \\ &\quad + \int_{y_0}^{x_0} dz I_\rho(x, z)\Pi_\rho(z, y), \end{aligned} \quad (73)$$

with

$$\begin{aligned} \Pi'_F(x, y) &= -\frac{1}{2} \left[F'_{ab}(x, y)F'_{ab}(x, y) \right. \\ &\quad \left. - \frac{g^2}{4} \rho_{ab}(x, y)\rho_{ab}(x, y) \right], \\ \Pi_\rho(x, y) &= -F'_{ab}(x, y)\rho_{ab}(x, y). \end{aligned} \quad (74)$$

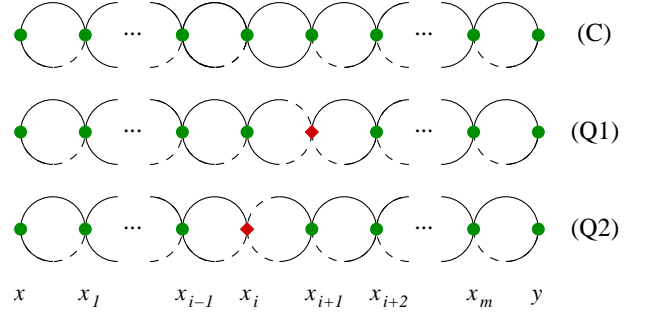


FIG. 2: (color online) Diagrammatic representation of the bubble chains contributing to the functions I'_F and I_ρ at next-to-leading order in the 2PI $1/\mathcal{N}$ expansion. The meaning of lines and vertices is explained in Fig. 1. The chains of type (Q1) and (Q2) only appear for a quantum system. Type (C) is present both in quantum and classical systems. These diagrams exhibit that in each term contributing to the functions I'_F and I_ρ , there is at most one loop involving two correlators F' or ρ . In the classical limit of quantum theory, the loops involving two spectral functions ρ are suppressed compared to those with two statistical functions F' .

The functions P'_F and P_ρ , which vanish if $\phi = 0$, will be discussed below. Iterating the integral equation (73) implies that the functions I'_F and I_ρ can be represented as a series of bubble chains, as shown in Fig. 2. A full line represents a statistical correlator, while a retarded (advanced) propagator line changes, from left to right, from full (broken) to broken (full), see Fig. 1.

The quantum and classical vertices are depicted analogously in Fig. 1(b). Connecting the correlators through the respective vertices, one finds which types of bubble chains appear. The classes of non-vanishing bubble chains shown in Fig. 2 confirm the structure of the functions $I'_F(x, y)$ and $I_\rho(x, y)$ which are determined by the integral equation (73): In each term contributing to the diagrammatic expansion of these functions there is at most one loop containing two F' or two ρ correlators, the latter resulting from either G^R or G^A . In addition to this one finds that only the loop containing two ρ correlators goes with the vertex which is present in the quantum case only. Hence, considering the classical dynamics, the $\sim g^2\rho^2$ terms are absent together with the ‘quantum’ vertex. For the same reasons, the contribution $\sim (g^2/4)[I_\rho(x, y) + P_\rho(x, y)]\rho_{ab}(x, y)$ to $\Sigma_{ab}^{F'}(x, y)$ is absent for the classical statistical theory.

We proceed by considering the functions P'_F and P_ρ , which are relevant for the case of a non-vanishing ϕ' . The classes of bubble chains appearing in the self-energy for $\phi' \neq 0$ are derived from those shown in Fig. 2, by replacing at most one full $F'_{ab}(x, y)$ line by the product $\phi'_a(x)\phi'_b(y)$ of mean fields. This means, that the pair of correlators in one loop are replaced by either of the combinations

$$\begin{aligned} H'_F(x, y) &= -\phi'_a(x)F'_{ab}(x, y)\phi'_b(y), \\ H_\rho(x, y) &= -\phi'_a(x)\rho_{ab}(x, y)\phi'_b(y). \end{aligned} \quad (75)$$

The functions P'_F and P_ρ entering the self-energies (72) then

read [35]:

$$\begin{aligned}
P'_F(x, y) = & - \left\{ H'_F(x, y) \right. \\
& - \int_{t_0}^{x_0} dz [H_\rho(x, z)I'_F(z, y) + I_\rho(x, z)H'_F(z, y)] \\
& + \int_{t_0}^{y_0} dz [H'_F(x, z)I_\rho(z, y) + I'_F(x, z)H_\rho(z, y)] \\
& - \int_{t_0}^{x_0} dz \int_{t_0}^{y_0} dv I_\rho(x, z)H'_F(z, v)I_\rho(v, y) \\
& + \int_{t_0}^{x_0} dz \int_{t_0}^{z_0} dv I_\rho(x, z)H_\rho(z, v)I'_F(v, y) \\
& \left. + \int_{t_0}^{y_0} dz \int_{z_0}^{y_0} dv I'_F(x, z)H_\rho(z, v)I_\rho(v, y) \right\}, \\
P_\rho(x, y) = & -g \left\{ H_\rho(x, y) \right. \\
& - \int_{y_0}^{x_0} dz [H_\rho(x, z)I_\rho(z, y) + I_\rho(x, z)H_\rho(z, y)] \\
& \left. + \int_{y_0}^{x_0} dz \int_{y_0}^{z_0} dv I_\rho(x, z)H_\rho(z, v)I_\rho(v, y) \right\}. \quad (76)
\end{aligned}$$

We observe that there are no differences in the functions P'_F and P_ρ in the classical statistical limit except for a dependence on modified I'_F and I_ρ , since the terms involving the mean field ϕ'_a correspond either to $(F')^2$ or to $F'\rho$ loops. This implies that the presence of a non-vanishing mean field ϕ' does not add characteristic 'quantum' terms to the dynamical equations of motion.

Moreover, the tadpole diagrams contain the classical vertex and the F' correlator only. This shows that the left hand sides of the quantum dynamic equations, Eqs. (50) and (45), do not contain any contribution proportional to the quantum vertex marked with a (red) square in Fig. 1(b). As a result, the dynamics in the Hartree-Fock-Bogoliubov [67, 68, 69] approximation is the same for the quantum and the classical statistical theory for same initial conditions. Differences arise, at most, in the self-energies $\Sigma^{F'}$ and Σ^ρ . We point out that, neglecting the right-hand sides of Eqs. (50), (45), these equations constitute a set of time-dependent HFB equations for the mean field and the two-point functions, cf., e.g. Refs. [36, 37]. In this approximation, the dynamics of ρ decouples from that of ϕ and F . Neglecting also F , Eq. (50) becomes the Gross-Pitaevskii equation. Quantum fluctuations play no role in these approximations. For this reason, HFB is commonly termed a mean-field theory [71].

Summarizing, one concludes that all equations (45), (50), (47), (72), (73), (74), (75), and (76) remain the same in the classical statistical limit except for differing expressions for

the statistical components of the self-energy

$$\begin{aligned}
\Sigma_{ab}^{F'}(x, y) & \xrightarrow{\text{classical limit}} - \left\{ I'_F(x, y)\phi'_a(x)\phi'_b(y) \right. \\
& \left. + [I'_F(x, y) + P'_F(x, y)]F'_{ab}(x, y) \right\}, \\
\Pi'_F(x, y) & \xrightarrow{\text{classical limit}} -\frac{1}{2}F'_{ab}(x, y)F'_{ab}(x, y), \quad (77)
\end{aligned}$$

replacing the respective expression in Eqs. (72) and (74). The classical statistical self-energies can be obtained from the respective quantum ones by dropping two spectral (ρ -type) components compared to two statistical (F -type) functions. For vanishing macroscopic field ϕ where $P_{F,\rho} = 0$ this corresponds to the result of Ref. [45]. Using the rescaled variables (70) and (71) the 'quantum' terms can be directly identified since they are the only g -dependent terms, which are absent in the classical statistical theory according to the above discussion. As a consequence, for the classical dynamics the effects of a larger coupling can always be compensated by changing the initial conditions such that Fg , as well as $\phi\sqrt{g}$, remain constant. This cannot be achieved once quantum corrections are taken into account, since they become of increasing importance with growing coupling or reduced initial values for F and ϕ .

2. 'Classicality' condition

Eq. (77) describes the differences between quantum and classical statistical equations of motion. In turn one can ask under which conditions these differences are negligible. In that case the quantum dynamics can be well approximated by classical statistical dynamics. To analyse this we iteratively expand Eq. (73) in terms of Π'_F and Π_ρ and compare term by term the statistical components of the quantum self-energies in Eqs. (72) and (74) to the respective classical ones according to (77). One finds that a sufficient condition for the suppression of quantum fluctuations compared to classical statistical fluctuations is given by

$$|F'_{ab}(x, y)F'_{cd}(z, w)| \gg \frac{3}{4}g^2 |\rho_{ab}(x, y)\rho_{cd}(z, w)|. \quad (78)$$

This condition is not based on thermal equilibrium assumptions and holds also for far-from-equilibrium dynamics. In particular, it is independent of the value of the macroscopic field ϕ . Our results, therefore, agree with previous $\phi = 0$ estimates in Refs. [44, 45]. We also note that the condition (78) is precisely the same as the one obtained from the 2PI loop expansion [34, 44].

The condition (78) can be applied, of course, also in thermal equilibrium, for which the statistical and spectral correlation functions are no longer independent quantities. In thermal equilibrium they are rather related to each other through the fluctuation-dissipation relation, which, for a homogeneous system in energy-momentum space, reads

$$F^{(\text{eq})'}(\omega, \mathbf{p}) = -ig \left(\frac{1}{2} + n(\omega, T) \right) \rho^{(\text{eq})}(\omega, \mathbf{p}), \quad (79)$$

with the Bose-Einstein distribution function $n(\omega, T) = (e^{(\omega-\mu)/k_B T} - 1)^{-1}$. For large temperatures, $k_B T \gg \omega - \mu$, one has $|F^{(\text{eq})'}(\omega, \mathbf{p})|/g \gg |\rho^{(\text{eq})}(\omega, \mathbf{p})|$, i.e., the classicality condition is fulfilled for all modes whose occupation number $\sim F^{(\text{eq})'}(\omega, \mathbf{p})/g$ is much larger than $\mathcal{O}(1)$. The equivalent statement can be directly derived from (78) also for nonequilibrium evolutions whenever it is possible to define a suitable 'occupation number' from a space-time or energy-momentum dependent proportionality between F and ρ . A nonequilibrium example will be discussed in Sect. III.

Away from equilibrium the situation is often considerably more complicated. Strictly speaking the condition (78) must be valid at all times and for all space points, or momenta in Fourier space, for the classical and the quantum evolution to agree. In practice, however, it needs only be fulfilled for time and space averages. In Sect. III we will demonstrate how quantum evolution can be approximated for not too late times by classical statistical dynamics, if the correlation functions satisfy (78) at initial time. In order to have quantum fluctuations playing a significant role, also for dynamically evolving gases, one either needs to increase the interaction strength g accordingly or change the phase-space structure by changing the external trapping potential. For example, in a one-dimensional trap, an effectively strong coupling and strong quantum fluctuations can be induced by reducing the line density of atoms while their interaction strength is kept constant. Such a case will be considered in Sect. III C below.

III. FAR-FROM-EQUILIBRIUM TIME EVOLUTION OF AN ULTRACOLD BOSE GAS

In this section we apply the theoretical methods summarized above to describe the equilibration dynamics of a uniform ultracold gas of bosonic sodium atoms which are confined such that they can move in one spatial dimension only. With present-day experimental technology, such a situation is achievable, e.g., using strong transversal confinement in an optical lattice or in a microtrap on the surface of a chip.

We will compare the evolution involving only classical statistical fluctuations with that which also takes into account quantum corrections. Both, the classical and the quantum gas are assumed to be initially characterized by the same initial conditions far from thermal equilibrium. For the quantum gas, the ensuing equilibration process is found to happen on two different time scales. A fast dephasing period leads to a quasistationary state which shows certain near-equilibrium characteristics but is still far from being thermal. After this, the system approaches, within an at least ten times longer period, the actual equilibrium state. On the contrary, the classical gas does not show the dephasing when considering the same initial mode occupation numbers as for the quantum gas. We show that the dephasing in the short-time evolution of the quantum gas can, to a certain extent, be simulated by a classical gas if one chooses the same initial values for the correlation functions. Our results show explicitly that quantum fluctuations only play a role for modes whose occupation number is sufficiently small. Hence, the dynamics of the weakly in-

teracting one-dimensional gas is almost purely classical. The long-time evolution is different in the classical and quantum cases, since only the latter can reach a Bose-Einstein distribution. We then study the example of a strongly interacting one-dimensional gas. For such a gas we find characteristic differences. For instance, for given identical initial values for the correlation functions, in the quantum evolution the decay of correlations with the initial state takes much longer as it would be expected from a calculation in the classical approximation.

A. Initial conditions

The 2PI effective action approach is convenient for situations, where at time $t = 0$ one has a Gaussian state, i.e., a state, for which all but the correlation functions of order one and two vanish [75]. In the following we will consider a one-dimensional uniform system, for which the two-point functions $F_{ab}(x, y)$ and $\rho_{ab}(x, y)$ are spatially translation invariant. We will therefore work in momentum space, where the kinetic energy operator is diagonal. Moreover, we choose the mean field ϕ to vanish initially. Then, for reasons of number conservation, the equations of motion (50) and (45) will conserve $\phi = 0$ for all times. We note that, since there is no spontaneous symmetry breaking in one spatial dimension at non-zero temperature, the field always approaches zero eventually, irrespective of its initial value.

Having prescribed initial values $F_{ab}(0, 0; p)$, with $\rho_{ab}(0, 0; p)$ given by Eq. (49), the coupled system of integro-differential equations (45) yields the time evolution of the two-point functions, in particular, of the momentum distribution

$$n(t, p) = \frac{1}{2} \left(F_{11}(t, t; p) + F_{22}(t, t; p) - \alpha \right). \quad (80)$$

For the quantum gas, one has $\alpha = 1$ from the Bose commutation relations, while, for a gas following classical statistical evolution, $\alpha = 0$.

We choose, at $t = 0$, a Gaussian momentum distribution

$$n(0, p) = \frac{n_1}{\sqrt{\pi}\sigma} e^{-p^2/\sigma^2}. \quad (81)$$

which constitutes a far-from-equilibrium state for the quantum gas as well as for the classical gas if the interactions are non-zero and the corresponding interaction energy is much larger than the kinetic energy.

The initial pair correlation function vanishes,

$$0 = \frac{1}{2} \left(F_{11}(t, t; p) - F_{22}(t, t; p) \right) + iF_{12}(t, t; p), \quad (82)$$

for $t = 0$, in accordance with total atom number conservation at non-relativistic energies [76]. Hence,

$$F_{11}(0, 0; p) = F_{22}(0, 0; p) = n(0, p) + \alpha/2, \quad (83)$$

$$F_{12}(0, 0; p) = F_{21}(0, 0; p) \equiv 0. \quad (84)$$

As far as the spectral functions are concerned, in the quantum case, the Bose commutation relations, and, in the classical case, the Poisson brackets require, cf. Eqs. (49), (65):

$$\rho_{11}(t, t; p) = \rho_{22}(t, t; p) \equiv 0, \quad (85)$$

$$-\rho_{12}(t, t; p) = \rho_{21}(t, t; p) \equiv 1. \quad (86)$$

We have investigated the dynamic evolution of a 1D Bose gas of sodium atoms in a box of length $L = N_s a_s$, with periodic boundary conditions. We choose the numerical grid such that it corresponds to a lattice of N_s points in coordinate space with grid constant a_s , and the momenta on the Fourier transformed grid are $p_n = (2/a_s) \sin(n\pi/N_s)$. The results presented in the following are obtained using $N_s = 64$ modes on a spatial grid with grid constant $a_s = 1.33 \mu\text{m}$. We first consider a line density of the atoms in the box of $n_1 = 10^7$ atoms/m. In this case the atoms are weakly interacting with each other, such that $g_{1D} = \hbar^2 \gamma n_1 / m$, with the dimensionless parameter $\gamma = 1.5 \cdot 10^{-3}$. The width of the initial momentum distribution is chosen to be $\sigma = 1.3 \cdot 10^5 \text{m}^{-1}$. In order to explore a strongly interacting gas we then reduce the total number of atoms by a factor of 100, increasing the dimensionless interaction parameter γ by 10^4 . Here it is important that we employ a nonperturbative approximation which is not based on weak interactions.

B. Equilibration of the quantum gas

To solve Eqs. (45), with the self-energies given by Eqs. (72), for the initial conditions given in the previous section, we have implemented a parallelized Runge-Kutta solver and used a cluster of 3 GHz dual processor PCs with up to one node per momentum mode. The correlation functions $F_{ab}(t, t'; p)$ and $\rho_{ab}(t, t'; p)$ were propagated, for fixed t' , along t , using a second-order Runge-Kutta algorithm. After each Runge-Kutta step, the $I_{F,\rho}$ integrals were updated according to Eqs. (73). The dynamic equations derived from the 2PI effective action are, by construction, number and energy conserving. While number conservation, by virtue of the $O(2)$ symmetry of each diagram, is given exactly, energy conservation may be violated by the chosen discretization along the time axis. Hence, in order to ensure optimal energy conservation numerically, a fourth-order Runge-Kutta algorithm was employed for the propagation of the correlation functions along the diagonal $t = t'$.

Fig. 3 shows, as a (red) solid curve, the initial Gaussian momentum distribution of the gas, on a logarithmic scale, where it forms an inverted parabola. The filled circles indicate the numerically calculated modes p_i . In the same figure, the time evolution of the distribution is shown for different times between $t = 0.1 \text{ms}$ and 0.6s . For times greater than about 0.15s , there is only very little change observed. As a function of time, the evolution of the single mode occupations is shown in Fig. 4. We observe that the system very quickly, after about $5 \mu\text{s}$, evolves to a quasistationary state, and that the subsequent drift to the equilibrium distribution takes roughly ten times longer. In passing we note that

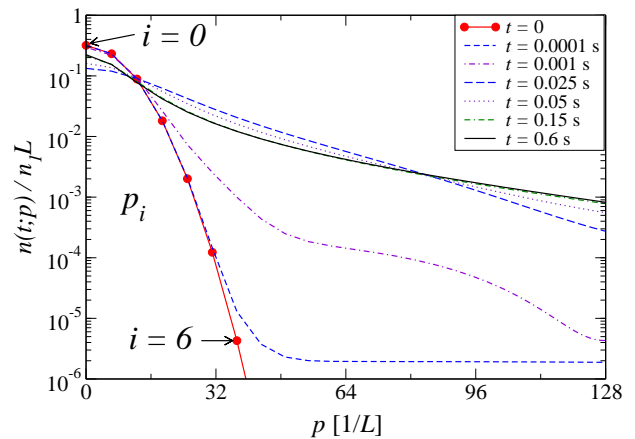


FIG. 3: (Color online) Momentum-mode distribution $n(t; p)$ for the initial state (red filled circles, interpolated by red solid line) and 6 subsequent times t until no change can be observed for $t > 0.6 \text{s}$. The interpolation of the final distribution is shown as a black solid curve. Note the logarithmic scale. The occupation numbers are normalized by the total number of atoms in the box, $n_1 L = 853$. The gas is in a far-from-equilibrium state initially, characterized by a Gaussian distribution $n(0; p)$, Eq. (81), with width $\sigma = 1.3 \cdot 10^5 \text{m}^{-1}$. It is weakly interacting, $\gamma = 1.5 \cdot 10^{-3}$. Since we consider a homogeneous gas and a symmetric initial state, the occupation numbers are invariant under $p \rightarrow -p$.

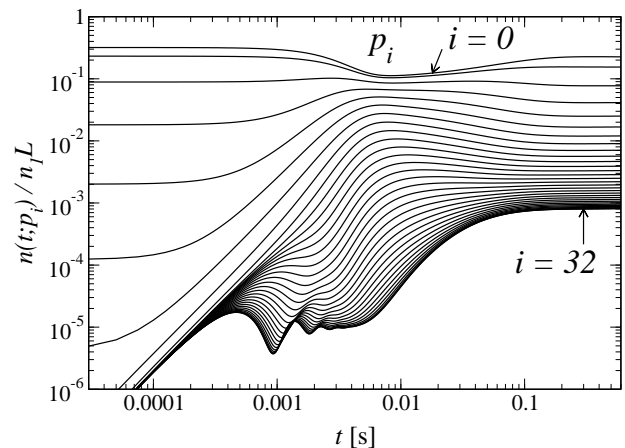


FIG. 4: The normalized momentum-mode occupation numbers $n(t; p)/n_1 L$, corresponding to those shown in Fig. 3, as functions of time. Shown are the populations of the modes with $p = p_i = 2N_s/L \sin(i\pi/N_s)$, $i = 0, 1, \dots, N_s/2$, and one has $n(t; -p) = n(t; p)$. A fast short-time dephasing period is followed by a long quasistationary drift to the final equilibrium distribution. Notice the double-logarithmic scale.

the mean-field Hartree-Fock (HF) approximation, for which $\Sigma^F = \Sigma^\rho \equiv 0$ in Eqs. (45), conserves exactly all mode occupations and no equilibration is seen.

In order to estimate to which extent the final distribution approaches that of the actual equilibrium state of the gas, we fitted the distribution to the Bose-Einstein-like form $n(t; p) = [\exp\{(\omega(p) - \mu)/k_B \Theta(t; p)\} - 1]^{-1}$, with a p -dependent temperature variable $\Theta(t; p)$. Here $\omega(p)$ was derived from

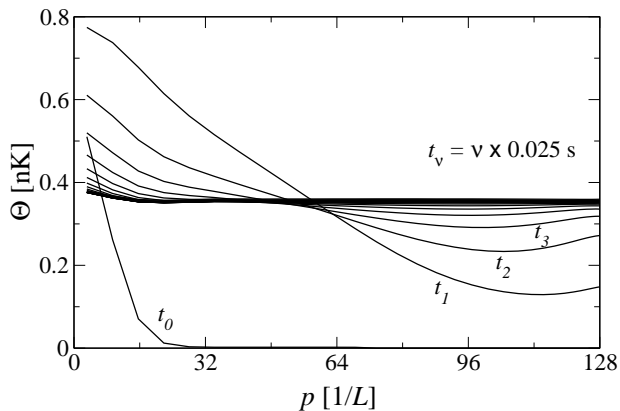


FIG. 5: Momentum and time dependent temperature variable $\Theta(t; p)$ obtained by fitting the distribution $n(t; p) = [\exp\{(\omega(p) - \mu)/k_B\Theta(t; p)\} - 1]^{-1}$ to the distribution obtained from the results shown in Fig. 4, for different, equally spaced times between $t = 0$ and $t = 0.6$ s. One observes that, during the quasistationary period, $0.01 \text{ s} < t < 0.1$ s, no temperature can be associated to the distribution. Only at very large times, Θ becomes approximately p -independent.

time-derivatives of the statistical function $F(t, t'; p)$ at $t = t'$. If a Bose-Einstein distribution is approached the temperature can be obtained from the slope of $\log(n^{-1} + 1)$ and the chemical potential μ from its value at $\omega = 0$. Fig. 5 shows $\Theta(t; p)$ for $t = 0 \dots 0.6$ s. Obviously, during the quasistationary drift period, no temperature can be attributed to $n(t; p)$, while, for large t , Θ becomes approximately p -independent [77]. We deduce an approximate final temperature from $\Theta(0.6 \text{ s}; 128/L) = T = 0.35 \text{ nK}$ with $\mu = 1.08 g_{1D} n_1$ for the above given values of g_{1D} and n_1 , which, hence, deviates from the HFB result $\mu = g_{1D} n_1$ by 8% only.

We furthermore studied, in the spirit of Refs. [70, 72], the time dependence of the ratio of the envelopes of the unequal-time correlation functions, specifically, $\xi(t; p) = [(F_{11}(t, 0; p)^2 + F_{12}(t, 0; p)^2)/(\rho_{11}(t, 0; p)^2 + \rho_{12}(t, 0; p)^2)]^{1/2}/n(t; p)$. Fig. 6 shows ξ , for four different momentum modes, as a function of time. Due to the normalization with respect to $n(t; p)$ all $\xi(t; p)$ are of the same order of magnitude. However, they show a distinct time evolution during the dephasing period, before they settle to a constant value during the quasistationary drift. ξ is a measure of the interdependence of the statistical and spectral functions, which, in thermal equilibrium, are connected through the fluctuation-dissipation relation [70]. In the momentum-frequency domain, this relation is given in Eq. (79). Hence, the stationary ξ indicates that F and ρ are linked to each other long before the momentum distribution becomes thermal.

A further signature is found when comparing the kinetic and interaction contributions to the total energy as shown in Fig. 7. During the quasistationary drift, these contributions are constant and of the same order of magnitude, calling in mind the virial theorem.

In summary, during the drift period, the system is not yet in equilibrium as far as the momentum distribution and temperature is concerned, but shows important characteristics of

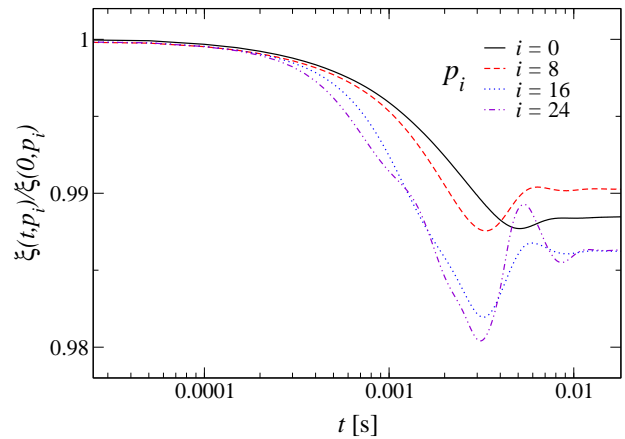


FIG. 6: (Color online) Ratio of the envelopes of the unequal-time correlation functions, $\xi(t; p) = [(F_{11}(t, 0; p)^2 + F_{12}(t, 0; p)^2)/(\rho_{11}(t, 0; p)^2 + \rho_{12}(t, 0; p)^2)]^{1/2}/n(t; p)$, for four different momentum modes, as a function of time. Due to the normalization with respect to $n(t; p)$ all $\xi(t; p)$ are of the same order of magnitude. ξ is a measure of the interdependence of the statistical and spectral functions, and its settling to a constant value during the quasistationary drift indicates that these functions become, as in thermal equilibrium, connected through a fluctuation-dissipation relation.

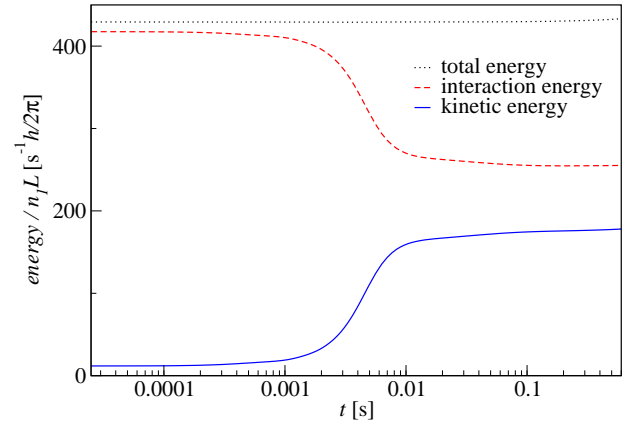


FIG. 7: (Color online) Evolution of the kinetic and interaction contributions to the total energy of the gas. During the quasistationary drift these contributions assume the same order of magnitude, calling in mind the virial theorem.

a system close to equilibrium.

C. Evolution of the classical gas

In Section II we have discussed in detail the distinction between the quantum and classical statistical contributions to the 2PI effective action and to the dynamic equations. In the following we compare the predictions for the classical statistical theory with those presented in the preceding section, and pointing to the distinct differences.

We solved Eqs. (45), with the self-energies now given by Eqs. (77), for the initial conditions given in Section III A, first

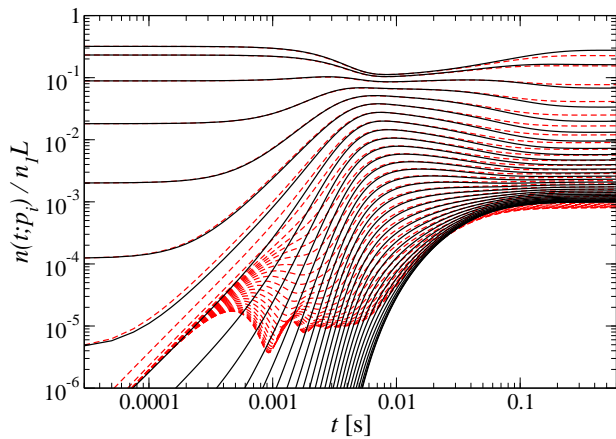


FIG. 8: (Color online) The normalized momentum-mode occupation numbers $n(t; p)/n_1 L$ for the classical gas (black solid lines) compared to their quantum counterparts from Fig. 4 (red dashed lines), as functions of time. Shown are the populations of the modes with $p = p_i = 2N_s/L \sin(i\pi/N_s)$, $i = 0, 1, \dots, N_s/2$, and one has $n(t; -p) = n(t; p)$. In contrast to the quantum statistical evolution there is no quick dephasing in the classical case, such that the initially empty modes become only subsequently filled, as is discussed in the main text. At large times, the classical and quantum gases necessarily evolve to different distributions.

with $\alpha = 0$. For comparison we also consider the case $\alpha = 1$ such that the classical and quantum initial correlation functions F and ρ are identical. In the classical case, the self-energies as well as the equations (73) determining the coupling functions $I_{F,\rho}$ are lacking certain terms compared to their quantum counterparts, cf. Eq. (77).

The time evolution of the initially Gaussian far-from-equilibrium momentum distribution of the classical gas is shown in Fig. 8. The mode occupations are shown as (black) solid lines, and for better comparison, we have quoted the quantum evolution from Fig. 4 as (red) dashed curves. One observes that the time evolution of the modes with occupation number $n(t; p) > 1$, i.e., $n(t; p)/n_1 L > 10^{-3}$, is, for most of the time, identical to that obtained in the quantum case, confirming condition (78). As expected, for the strongly populated modes of a weakly interacting bosonic gas quantum fluctuations do not play a significant role for not too large times. Only when the evolution approaches the equilibrium state, the differences between quantum and classical statistics are expected to lead to a Bose-Einstein and classical distribution, respectively. We point out that, although we have chosen, for our comparison, the same initial occupation numbers in the two cases, the total energies are different since the initial correlation functions differ according to Eq. (83). Hence, also the final-state occupation numbers of the low momentum modes can differ.

We finally point to the substantial differences in the short-time evolution of the weakly populated modes. While, in the quantum gas, the large-momentum mode populations are all growing at the same rate, the modes of the classical gas become populated much more gradually. The quantum-gas modes are occupied by 0.01 and 1 particle per mode already

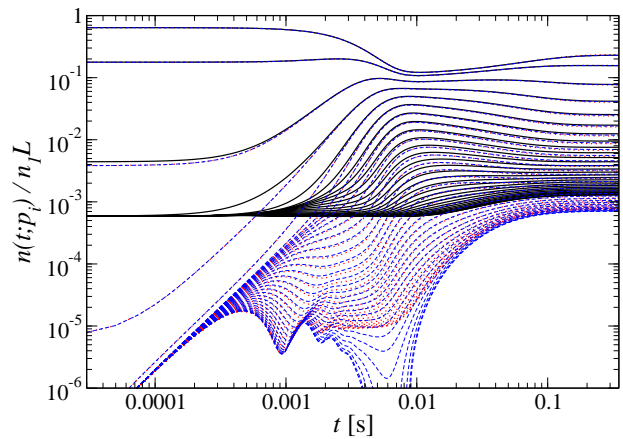


FIG. 9: (Color online) The normalized momentum-mode occupation numbers $n(t; p)/n_1 L$ for the classical gas (black solid lines) compared to their quantum counterparts from Fig. 4 (red dotted lines), as functions of time. All parameters are chosen as in Fig. 8, except for $\sigma = 6.5 \cdot 10^4 \text{ m}^{-1}$. The dashed (blue) lines show $n(t, p) - 1/2$, i.e., after subtracting the additional flat initial distribution which simulates the quantum “zero point fluctuations”.

between 0.5 and 1 μs , while the classical modes need up to ten times longer. The distinct quantum behaviour of the modes can be understood as follows. At the energies present in such an ultracold gas, the atomic interactions are essentially pointlike, i.e., the range of the potential is not resolved and the coupling function or scattering amplitude is constant over the range of relevant momenta. Hence, in a single scattering event, the distance of two atoms is localized to zero, such that the relative momentum of the atoms is completely unknown immediately after the collision. This means that the transfer probability of the atoms is the same for any final momentum mode, and this is observed as a quick, collective population in the respective, so far essentially unoccupied modes.

For comparison we repeated our calculations for a non-local interaction potential. In the momentum domain, this corresponds to a coupling function which is cut off at large momenta, and we chose the cutoff within the range of the momenta shown explicitly in Fig. 8. In this case we find that the quantum evolution is modified such that it becomes similar to that of the classical gas. In particular, all modes above the cutoff populate gradually one after each other.

The differences between the quantum and classical evolutions shown above depend, however, considerably on the choice of initial conditions. To compare the characteristics of the evolutions which are independent of the initial choice of F , we have repeated the classical calculations for an initial momentum distribution where, as compared to before, a constant occupation number 1/2 has been added. Hence, we chose $\alpha = 1$ in the initial values of F , Eq. (83), as in the quantum case, such that F is identical for $x_0 = y_0 = t_0$ in the classical and quantum cases. The results are shown in Fig. 9. The (red) dotted lines show, again, the quantum evolution, while the classical mode populations for the same initial conditions for F and ρ are shown as solid (black) lines. Subtracting 1/2 from each $F_{aa}(t, t; p)$ gives the dashed (blue) lines. We find,

that during the initial period the evolution of the variation of the high-momentum modes with respect to their initial occupation is identical to the quantum evolution of the occupation numbers. At intermediate times, however, there are deviations which lead to occupation numbers up to a percent lower than 1/2. Although the chosen initial conditions which, in the classical case correspond to a base occupation of each mode with 1/2 atom, seem unphysical, our results show that for the dilute, weakly interacting gas under consideration, there are differences only in those modes which, in the mean, are populated with less than one atom. Quantum statistical fluctuations play a role only for these modes.

The situation is very different for an ultracold gas in the strongly interacting regime. We obtain this from the case discussed so far by reducing the total number of atoms by a factor of 100 and increasing the dimensionless interaction parameter γ by 10^4 . In this case the 'classicality' condition (78) is clearly violated and we expect strong corrections due to quantum fluctuations. We emphasize that here our nonperturbative approximation is crucial in order to be able to consider such strongly interacting systems. Note that the structure of the classical equations of motion, Eqs. (45), with the self-energies given by Eqs. (77), is such that they are invariant under a simultaneous rescaling of γ and n_1 which leaves γn_1^2 unchanged. The quantum equations will, however change, with the specific quantum terms becoming more and more important with growing γ and reduced density n_1 . We compare the evolution, again, for identical initial conditions as in the case shown in Fig. 9. The deviations between quantum and classical statistical evolution are now quantitatively substantial. While many qualitative aspects are similar to those discussed above, now all momentum modes show clear deviations. As a characteristic example, we present, in Fig. 10, the ratio of the envelopes of the unequal-time correlation functions, in analogy to Fig. 6, for the quantum and classical evolution of the strongly interacting gas. One observes that the unequal-time correlation function decays more rapidly in the classical statistical case. Our results illustrate that the quantum system keeps much longer the information about the initial conditions, here roughly by an order of magnitude in evolution time. On the other hand, the example also shows that the classical statistical system still behaves qualitatively similar to the quantum gas, despite the low densities and strong interactions. We would like to emphasize that clearly distinguishing quantum and classical statistical fluctuations will typically require high precision, both from the calculational as well as experimental point of view.

IV. CONCLUSIONS

In this article we have studied the non-equilibrium dynamics of an ultracold Bose gas and compared the theoretical predictions from a full quantum approach with those where only classical statistical fluctuations were taken into account. On the basis of functional techniques in quantum field theory we reviewed the difference in the generating functionals, the 2PI effective actions which determine the dynamic equations, be-

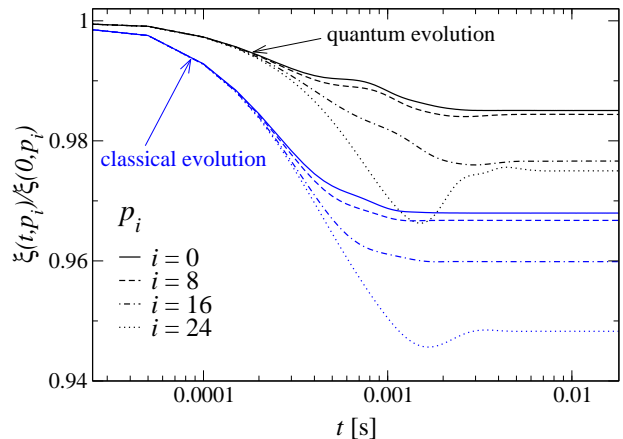


FIG. 10: (Color online) Ratio of the envelopes of the unequal-time correlation functions, $\xi(t; p) = [(F_{11}(t, 0; p)^2 + F_{12}(t, 0; p)^2) / (\rho_{11}(t, 0; p)^2 + \rho_{12}(t, 0; p)^2)]^{1/2} / n(t; p)$, for four different momentum modes, as a function of time. This figure is analogous to Fig. 6, but shows the difference of the quantum (black lines) and classical (blue lines) evolutions for a gas in the strongly correlated regime $\gamma = 15$, for $n_1 = 10^5 \text{ m}^{-3}$. The results show that in this regime, where quantum and classical statistical evolution differ considerably, the quantum evolution conserves information about the initial conditions much longer, here roughly by an order of magnitude in time.

tween the quantum and the classical cases. The functional descriptions for both cases show to be very similar. In particular, the crucial difference is the absence, in the classical versus the quantum case, of certain coupling terms or vertices in the action which defines the theory and which enters the generating functional of correlation functions. As a consequence, the classical generating functional is characterized by an important reparametrization property, such that for the classical dynamics the effects of a larger self-interaction can always be compensated by a smaller density. Quantum corrections violate this invariance property. They become of increasing importance with growing scattering length or reduced density. We have used this to derive a 'classicality' condition, which is not based on thermal equilibrium assumptions and holds also for far-from-equilibrium dynamics. In particular, it is independent of the value of the macroscopic field ϕ .

To illustrate the possibilities one has at hand, we studied the equilibration dynamics of a homogeneous ultracold gas of interacting sodium atoms in one spatial dimension. The gas is assumed to be, initially, in a state far from thermal equilibrium, characterized by a Gaussian momentum distribution centred at zero momentum. Extending on earlier results [36] we find that the evolution takes place via two distinct periods, with a fast initial dephasing followed by a slow quasistationary drift to the final equilibrium distribution. While the gas, during the quasistationary drift, already shows important characteristics of a near-equilibrium situation like a fluctuation-dissipation relation and constancy of the total kinetic energy, no temperature can yet be associated to the momentum distribution.

We compared this evolution to the evolution of a classi-

cal gas with different initial conditions. If the initial mode occupation numbers are chosen as in the quantum case, no short-time dephasing period is found. The modes are rather populated subsequently, with the quasistationary drift setting in gradually. The long-time approach to the final equilibrium state expectedly shows a distinct behaviour compared to the quantum gas. We moreover showed that the dephasing in the short-time evolution of the quantum gas can be approximately simulated by a classical gas if one chooses appropriate initial conditions. Our results demonstrate explicitly that quantum fluctuations only play a role for modes whose occupation number is sufficiently small. We found that the dynamics of the weakly interacting one-dimensional gas is almost purely classical. In contrast, for a strongly interacting one-dimensional gas we observed substantial quantitative deviations. There are distinctive properties of quantum versus classical statistical dynamics, as e.g. that, given identical initial values for the correlation functions, in the quantum evolution, information about the initial conditions is conserved much longer as it would be expected from a calculation in classical approximation. Such differences may be expected to be of interest in the context of strongly correlated ultracold atomic gases, e.g. in lower-dimensional traps or near Feshbach scattering resonances. However, we emphasize that high precision measurements together with accurate calculations are typically required to be able to clearly distinguish between effects of quantum and classical statistical fluctuations. We think that the nonperturbative methods presented here can be a very valuable tool to precisely identify the effect of quantum fluctuations on the time evolution of ultracold quantum gases observed in present-day and near-future experiments.

Acknowledgments

We thank Gert Aarts for collaboration on related work, and Hrvoje Buljan, Thorsten Köhler, Markus Oberthaler, Jan Martin Pawłowski, Jörg Schmiedmayer, Gora Shlyapnikov, and Kristan Temme for inspiring and valuable discussions, and Werner Wetzel for his continuing support concerning computers. This work has been supported by the Deutsche Forschungsgemeinschaft.

APPENDIX A: INITIAL CONDITIONS

In this appendix we provide explicit expressions for a general Gaussian initial-state density matrix $\rho_D[\varphi_0 + \tilde{\varphi}_0/2, \varphi_0 - \tilde{\varphi}_0/2]$ and a Gaussian probability functional $W[\varphi_0, \pi_0]$ entering the generating functionals (18) and (58), respectively. These specify the initial conditions for the dynamic equations (45), (50). We provide expressions for a spatially homogeneous system, as considered in Sect. III.

The most general Gaussian initial density matrix takes, in

the representation (12) of the fields, the form

$$\rho_D[\varphi_0 + \tilde{\varphi}_0/2, \varphi_0 - \tilde{\varphi}_0/2] = \frac{1}{2\pi\xi_1\xi_2} \exp \left\{ -\tilde{\varphi}_{0,a}\sigma_{ab}^2\phi_{0,b} - \frac{1}{2\xi_a^2}(\varphi_{0,a} - \phi_{0,a})^2 + i\frac{\eta_a}{\xi_a}(\varphi_{0,a} - \phi_{0,a})\tilde{\varphi}_{0,a} - \frac{\sigma_a^2}{8\xi_a^2}\tilde{\varphi}_{0,a}^2 \right\}, \quad (\text{A1})$$

where summation over a and b is implied in the exponent. Since ρ_D involves a factor of the above form above for each momentum mode, mode indices at the fields and parameters, as well as summation over momenta in the exponent have been neglected. In order to reflect the symmetry (6) between the field and the canonical momentum, the six parameters ξ_a , η_a , and σ_a are reduced to three independent parameters through the conditions

$$\begin{aligned} \sigma_1 &= \sigma_2 \equiv \sigma, \\ \xi_1^2 &= \eta_1^2 + \sigma^2/4\xi_2^2, \\ \eta_1 &= -\eta_2\xi_2/\xi_1. \end{aligned} \quad (\text{A2})$$

Using the definition of the initial statistical correlation functions in terms of the initial density matrix,

$$F_{ab}(0, 0) = \frac{1}{2} \text{Tr} \left[\rho_D(t_0) \{ \Phi_a(0), \Phi_b(0) \} \right] - \phi_{0,a}\phi_{0,b}, \quad (\text{A3})$$

and inserting unit operators $\int [d\varphi] |\varphi\rangle\langle\varphi|$ and/or $\int [d\pi] |\pi\rangle\langle\pi|$ one finds that the three free parameters are related to the initial correlation functions as follows

$$\begin{aligned} \xi_1^2 &= F_{11}(t_0, t_0) - \phi_{0,1}\phi_{0,1}, \\ \xi_1\eta_1 &= F_{12}(t_0, t_0) - \phi_{0,1}\phi_{0,2}, \\ \eta_1^2 + \sigma_1^2/4\xi_1^2 &= F_{22}(t_0, t_0) - \phi_{0,2}\phi_{0,2}. \end{aligned} \quad (\text{A4})$$

Again, all mode labels have been suppressed. The initial spectral functions $\rho_{ab}(0, 0)$ do not enter the density matrix as they are fixed, in the quantum and classical statistical cases, by the commutation relations and the Poisson brackets, respectively.

Note that the initial conditions chosen in Sect. III A for the numerical evaluation of the dynamics of a one-dimensional Bose gas, with $F_{11}(0, 0) = F_{22}(0, 0)$, $F_{12}(0, 0) = 0$ and $\phi_{0,a} \equiv 0$ correspond to $\xi_1^2 = \xi_2^2 \equiv \xi^2 = F_{11}(0, 0)$, $\eta_a = 0$, $\sigma = 2\xi^2$, such that

$$\begin{aligned} \rho_D[\varphi_0 + \tilde{\varphi}_0/2, \varphi_0 - \tilde{\varphi}_0/2] &= \frac{1}{2\pi\xi^2} \exp \left\{ -\frac{1}{2\xi^2}\varphi_{0,a}^2 - \frac{\xi^2}{2}\tilde{\varphi}_{0,a}^2 \right\}. \end{aligned} \quad (\text{A5})$$

We close this appendix by providing the expression for the probability functional $W[\varphi_0, \pi_0]$ obtained through the inverse of the Fourier transform (59):

$$\begin{aligned} W[\varphi_0, \pi_0] &= \frac{1}{\pi^2\sigma^2} \exp \left\{ -\frac{2\xi_a^2}{\sigma^2} \left(\frac{\eta_a}{\xi_a}\varphi_{0,a} - \pi_{0,a} \right)^2 - \frac{1}{2\xi_a^2}\varphi_{0,a}^2 \right\}. \end{aligned} \quad (\text{A6})$$

(Summation over a in the exponent). It is straightforward to show that the above expression is symmetric under exchange of $\varphi_{0,a}$ and $\pi_{0,a}$, and that, by inserting $\pi_{0,a} = i\sigma_{ab}^2\varphi_{0,b}$, one obtains the expression

$$W[\varphi_0] = \frac{1}{(2\pi)^2|F_{ab}|} \exp \left\{ -\frac{1}{|F_{ab}|} \left[F_{11}(0,0)\varphi_{0,2}^2 + F_{22}(0,0)\varphi_{0,1}^2 - 2F_{12}(0,0)\varphi_{0,1}\varphi_{0,2} \right] \right\}, \quad (\text{A7})$$

with $|F_{ab}| \equiv F_{11}(0,0)F_{22}(0,0) - F_{12}(0,0)F_{21}(0,0)$.

-
- [1] E. A. Cornell and C. E. Wieman, *Rev. Mod. Phys.* **74**, 875 (2002).
- [2] A. J. Leggett, *Rev. Mod. Phys.* **73**, 307 (2001).
- [3] F. Dalfovo, S. Giorgini, L. P. Pitaevskii, and S. Stringari, *Rev. Mod. Phys.* **71**, 463 (1999).
- [4] W. Ketterle, D. S. Durfee, and D. M. Stamper-Kurn, in *Proceedings of the International School of Physics - Enrico Fermi*, edited by M. Inguscio, S. Stringari, and C. E. Wieman (IOS Press, 1999), p. 67.
- [5] W. Ketterle, *Phys. Today* **52**, 30 (1999).
- [6] C. A. Regal, M. Greiner, and D. S. Jin, *Phys. Rev. Lett.* **92**, 040403 (2004).
- [7] H. T. C. Stoof and M. Houbiers, in *Proceedings of the International School of Physics "Enrico Fermi" on Bose-Einstein condensation in Varenna 1998*, edited by M. Inguscio, S. Stringari, and C. E. Wieman (IOS Press, Amsterdam, 1999), p. 175.
- [8] R. Grimm, in *Proceedings of the International School of Physics - Enrico Fermi, Course CLXIV, Varenna, 2006*, edited by M. Inguscio, W. Ketterle, and C. Salomon (eprint cond-mat/0703091, 2007).
- [9] E. P. Gross, *Nuovo Cim.* **20**, 454 (1961).
- [10] L. P. Pitaevskii, [*Zh. Eksp. Teor. Fiz.* 40, 646 (1961)] *Sov. Phys. JETP* **13**, 451 (1961).
- [11] M. J. Davis, S. A. Morgan, and K. Burnett, *Phys. Rev. A* **66**, 053618 (2002).
- [12] M. Köhl, M. J. Davis, C. W. Gardiner, T. Hänsch, and T. Esslinger, *Phys. Rev. Lett.* **88**, 080402 (2002).
- [13] M. J. Davis and C. W. Gardiner, *J. Phys. B* **35**, 733 (2002).
- [14] W. C. Stwalley, *Phys. Rev. Lett.* **37**, 1628 (1976).
- [15] E. Tiesinga, A. Moerdijk, B. J. Verhaar, and H. T. C. Stoof, *Phys. Rev. A* **46**, R1167 (1992).
- [16] E. Tiesinga, B. J. Verhaar, and H. T. C. Stoof, *Phys. Rev. A* **47**, 4114 (1993).
- [17] K. Burnett, *Nature (London)* **392**, 125 (1998).
- [18] T. Köhler, K. Góral, and P. S. Julienne, *Rev. Mod. Phys.* **78**, 1311 (2006).
- [19] D. S. Petrov, C. Salomon, and G. V. Shlyapnikov, *Phys. Rev. A* **71**, 012708 (2005).
- [20] M. W. Zwierlein, C. A. Stan, C. H. Schunck, S. M. F. Raupach, A. J. Kerman, and W. Ketterle, *Phys. Rev. Lett.* **92**, 120403 (2004).
- [21] M. Bartenstein, A. Altmeyer, S. Riedl, S. Jochim, C. Chin, J. H. Denschlag, and R. Grimm, *Phys. Rev. Lett.* **92**, 120401 (2004).
- [22] J. Schmiedmayer and R. Folman, *C. R. Acad. Sci. Paris IV* **2**, 333 (2001).
- [23] L. P. Pitaevskii and S. Stringari, *Bose-Einstein Condensation* (Clarendon Press, 2003).
- [24] D. Jaksch, C. Bruder, J. I. Cirac, C. W. Gardiner, and P. Zoller, *Phys. Rev. Lett.* **81**, 3108 (1998).
- [25] I. Bloch, *Phys. World* **17**, 25 (2004).
- [26] D. van Oosten, P. van der Straten, and H. T. C. Stoof, *Phys. Rev. A* **63**, 053601 (2001).
- [27] M. Greiner, O. Mandel, T. Esslinger, T. W. Hänsch, and I. Bloch, *Nature (London)* **415**, 39 (2002).
- [28] L. Tonks, *Phys. Rev.* **50**, 955 (1936).
- [29] M. Girardeau, *J. Math. Phys. (NY)* **1**, 516 (1960).
- [30] B. Paredes, A. Widera, V. Murg, O. Mandel, S. Fölling, I. Cirac, G. V. Shlyapnikov, T. W. Hänsch, and I. Bloch, *Nature (London)* **429**, 277 (2004).
- [31] J. M. Cornwall, R. Jackiw, and E. Tomboulis, *Phys. Rev. D* **10**, 2428 (1974).
- [32] J. M. Luttinger and J. C. Ward, *Phys. Rev.* **118**, 1417 (1960).
- [33] G. Baym, *Phys. Rev.* **127**, 1391 (1962).
- [34] J. Berges, *Nucl. Phys. A* **699**, 847 (2002).
- [35] G. Aarts, D. Ahrensmeier, R. Baier, J. Berges, and J. Serreau, *Phys. Rev. D* **66**, 045008 (2002).
- [36] T. Gasenzer, J. Berges, M. G. Schmidt, and M. Seco, *Phys. Rev. A* **72**, 063604 (2005).
- [37] A. Rey, B. Hu, E. Calzetta, A. Roura, and C. Clark, *Phys. Rev. A* **69**, 033610 (2004).
- [38] K. Temme and T. Gasenzer, *Phys. Rev. A* **74**, 053603 (2006).
- [39] J. Berges and J. Serreau, *Phys. Rev. Lett.* **91**, 111601 (2003).
- [40] F. Cooper, J. F. Dawson, and B. Mihaila, *Phys. Rev. D* **67**, 056003 (2003).
- [41] A. Arrizabalaga, J. Smit, and A. Tranberg, *JHEP* **10**, 017 (2004).
- [42] J. Berges, S. Borsányi, and J. Serreau, *Nucl. Phys. B* **660**, 51 (2003).
- [43] J. Berges, S. Borsányi, and C. Wetterich, *Phys. Rev. Lett.* **93**, 142002 (2004).
- [44] J. Berges, eprint hep-ph/0409233; *AIP Conf. Proc.* **739**, 3 (2005).
- [45] G. Aarts and J. Berges, *Phys. Rev. Lett.* **88**, 041603 (2002).
- [46] J. Berges, *Nucl. Phys. A* **702**, 351 (2002), hep-ph/0201204.
- [47] E. Hopf, *J. Ratl. Mech. Anal.* **1**, 87 (1952).
- [48] P. C. Martin, E. D. Siggia, and H. A. Rose, *Phys. Rev. A* **8**, 423 (1973).
- [49] P. C. Hohenberg and B. I. Halperin, *Rev. Mod. Phys.* **49**, 435 (1977).
- [50] R. Phythian, *J. Phys. A* **8**, 1423 (1975).
- [51] C. De Dominicis, *J. Phys. (Paris) C* **1**, 247 (1976).
- [52] H.-K. Janssen, *Z. Phys. B* **23**, 377 (1976).
- [53] R. Bausch, H. K. Janssen, and H. Wagner, *Z. Phys. B* **24**, 113 (1976).
- [54] R. Phythian, *J. Phys. A* **10**, 777 (1977).
- [55] C. De Dominicis and L. Peliti, *Phys. Rev. B* **18**, 353 (1978).
- [56] J. Schwinger, *J. Math. Phys.* **2**, 407 (1961).
- [57] L. V. Keldysh, [*Sov. Phys. JETP* **20**, 1018 (1965)] *Zh. Eksp. Teor. Fiz.* **47**, 1515 (1964).
- [58] G. Zhou, Z. Su, B. Hao, and L. Yu, *Phys. Rev. B* **22**, 3385

- (1980).
- [59] G. Chou, Z. Su, B. Hao, and L. Yu, Phys. Rep. **118**, 1 (1985).
- [60] K. B. Blagoev, F. Cooper, J. F. Dawson, and B. Mihaila, Phys. Rev. D **64**, 125003 (2001).
- [61] G. Aarts and J. Smit, Phys. Lett. B **393**, 395 (1997).
- [62] W. Buchmüller and A. Jakovác, Phys. Lett. B **407**, 39 (1997).
- [63] G. Aarts and J. Smit, Nucl. Phys. B **511**, 451 (1998).
- [64] F. Cooper, A. Khare, and H. Rose, Phys. Lett. B **515**, 463 (2001).
- [65] C. Wetterich, Phys. Rev. E **56**, 2687 (1997), hep-th/9703006.
- [66] S. Jeon, Phys. Rev. C **72**, 014907 (2005).
- [67] D. R. Hartree, Proc. Cambridge Phil. Soc. **24**, 89 (1928).
- [68] V. Fock, Z. Phys. **61**, 126 (1930).
- [69] N. N. Bogoliubov, J. Phys. (USSR) **11**, 23 (1947).
- [70] G. Aarts and J. Berges, Phys. Rev. D **64**, 105010 (2001).
- [71] A. L. Fetter and J. D. Walecka, *Quantum theory of many-particle systems* (MacGraw-Hill, New York, 1971).
- [72] J. Berges and J. Cox, Phys. Lett. **B517**, 369 (2001).
- [73] J. Berges, Phys. Rev. D **70**, 105010 (2004).
- [74] In Ref. [36] we used the notation $iG_0^{-1}(\phi \equiv 0) = iD^{-1}$.
- [75] In the case that, at $t = 0$, the n th-order connected correlation function $\langle \Phi_{a_1}(0, \mathbf{x}_1) \cdots \Phi_{a_n}(0, \mathbf{x}_n) \rangle_c$ is non-zero, with all m th-order functions, $m > n$, vanishing, a straightforward generalization of the approach involving the n PI effective action is at hand [73].
- [76] At non-relativistic energies, the total number of atoms in a finite system is fixed such that correlation functions defined as expectation values of a field operator product with an unequal number of creation and annihilation operators vanish identically.
- [77] A rigorous calculation of the final temperature can be based on the Bose-Einstein distribution defined in energy-momentum space, which may be extracted using the fluctuation-dissipation (79) at late times along the lines of Ref. [42].